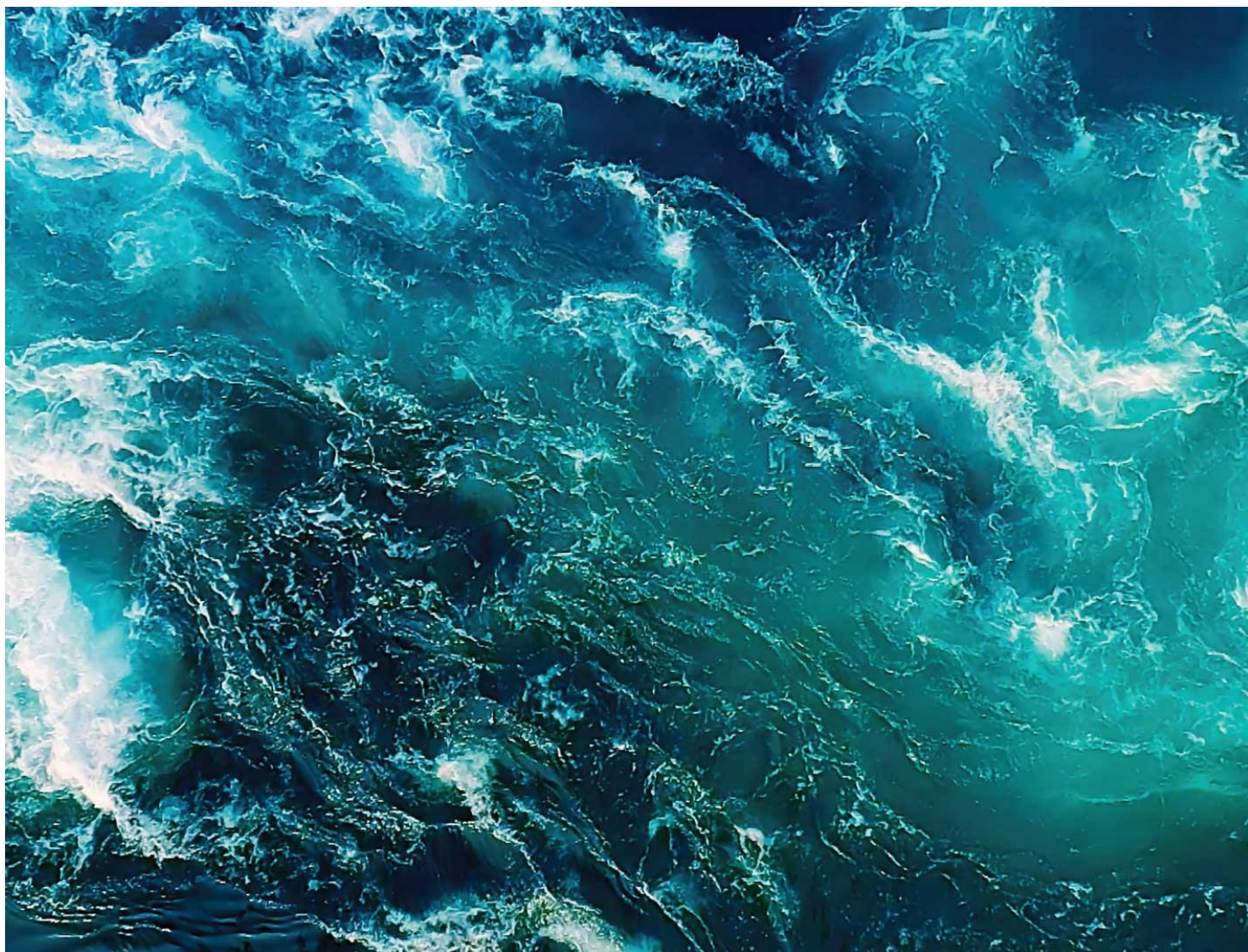


# Glider study at Hywind Scotland

Final report



<b>Report</b> Glider study at Hywind Scotland	
<b>Author(s):</b> Virginie Ramasco	Akvaplan-niva report: 2021 62861.01
	<b>Date:</b> 30-03-2022
	<b>Pages:</b> 46
	<b>Distribution:</b> Confidential
<b>Client:</b> Equinor Energy AS	<b>Client's reference</b>
<b>Summary</b> <p>The potential reef-effect of a floating wind park (Hywind Scotland, Equinor) was investigated by means of echosounder sampling on a distance gradient from the farm with an autonomous vehicle, the Sailbuoy. The temporal and spatial patterns highlighted in this work suggest that the installations likely have an effect on the low trophic levels (primary and secondary producers) in boosting production and consequently increasing standing stock, which in turn triggers fish aggregations. The results, on the other hand, do not support the theory of consistent increased fish biomasses in the vicinity of the park over time, but rather a stronger response to the natural occurrence of phytoplankton bloom and subsequent trophic cascade.</p> <p>While a time lag between phytoplankton and zooplankton increase has been observed in this study, the high aggregation of fish was nearly simultaneous with the zooplankton increase, indicating that fish responded fast, likely by moving towards the areas of high zooplankton concentration for feeding.</p> <p>The current project showed the successful use of remotely operated glider technology for environmental monitoring of fish aggregations around installations at sea.</p>	
<b>Project manager</b>  Virginie Ramasco	<b>Quality controller</b>  Lionel Camus, Paul Renaud

## Table of Content

1 INTRODUCTION .....	4
1.1 Objectives & scientific questions .....	4
1.2 Background.....	4
1.2.1 Reef-effect of offshore wind farms .....	4
1.2.2 Day/night variation of reef-effect .....	4
1.3 Approach .....	4
2 MATERIAL & METHODS .....	6
2.1 Selected technology .....	6
2.1.1 Platform .....	6
2.1.2 Sensors.....	6
2.1.3 Sensors' settings.....	6
2.2 Sampling campaign .....	7
2.3 Sampling area and risk mitigation .....	9
2.4 Data analysis.....	10
2.4.1 Echo sounder data analysis approach .....	10
2.4.2 Noise removal.....	11
2.4.3 Biomass detection and classification .....	12
2.4.4 Choice of indicators.....	13
2.5 Distance gradient from the park .....	13
2.6 Environmental and human factors .....	15
2.6.1 Marine traffic and fisheries.....	15
2.6.2 Bottom depth and light regime .....	15
2.7 Statistical analysis and spatial interpolation.....	15
3 RESULTS & DISCUSSION .....	16
3.1 Interpretation of figures .....	16
3.2 Data sampled .....	16
3.3 Effect of environmental factors on fish biomass, density and vertical migration .....	18
3.3.1 Bottom depth .....	18
3.3.2 Diel vertical migration.....	21
3.4 Spatial and temporal trends with distance to the infrastructures .....	24
3.4.1 Oceanographic conditions and phytoplankton bloom .....	24
3.4.2 Succession patterns.....	26
3.4.3 Effect of the distance from the park .....	29
3.4.4 Disturbance sources .....	31
4 CONCLUSIONS .....	32
4.1 Is there a reef-effect at Hywind Scotland? .....	32
4.2 Suitability of the approach for offshore wind parks .....	34
4.3 Suggestions for future investigations/applications .....	35
5 REFERENCES .....	36
6 APPENDIX .....	38

# 1 Introduction

---

## 1.1 Objectives & scientific questions

Equinor has developed and implemented the world's first floating offshore wind farm, composed of five floating wind turbines, off the coast of Peterhead, Scotland. In order to identify whether the infrastructures generate a "reef-effect" (i.e. increased aggregations due to attraction or increased productivity) on local fish population, Akvaplan-niva AS was contracted to collect information on fish stock at and around the wind farm. In this report, we present the methodologies and the results, along with a discussion on the potential reef-effect of this particular farm and concluding remarks on the use of the autonomous technology used for this particular experiment.

## 1.2 Background

### 1.2.1 Reef-effect of offshore wind farms

Although there are many methodological and ecological challenges associated with studies testing a potential reef-effect of artificial installations at sea, significantly increased abundance of certain fish species in the vicinity of offshore wind farms has been observed (e.g. Lindeboom et al. 2011, and citations therein). In the North Sea, Cod (*Gadus morhua*) and pouting (*Trisopterus luscus*) were shown to be attracted by wind farms in summertime. Tagged cod were mostly observed less than 100 m from these farms, and 90% of the observations were made <40m m from the turbines (note that hard substrates extended ~25 m from the turbine; Vandendriessche et al. 2013). Moreover, from December to March, tagged cod were barely observed close to the turbines, whereas some registrations were recorded in springtime. Close to the wind turbines, the abundance was up to 100 times that of the reference area. Very weak/non-existing reef-effect was observed between the windmills (>180 m from the structures, Vandendriessche et al. 2013). Fauna living on the structures (e.g., amphipods) has been shown to attract large schools of juvenile whiting. Wind turbine structures attract cod and pouting to a much greater extent than shipwrecks (Reubens et al. 2014). Tagged fish show a strong site fidelity, being found close to the wind turbines 75% of the time in summer and autumn.

### 1.2.2 Day/night variation of reef-effect

Although little evidence is available, an experiment was conducted in the vicinity of an oil platform in the North Sea (Soldal et al 1998). This study indicated more frequent appearance of tagged cod in night-time than in daytime, possibly due to the attractive effect of light emitted from the platform in night-time. On the other hand, *Ammodytes spp.* are known to be attracted by wind turbines, but rest buried in seabed sediments in night-time and feed in the upper water masses in daytime. Indeed, fish were mostly found close to the wind turbines in daytime (e.g., using the structures as shelter), moving to deeper waters further away from the turbines in night-time (Leonhard et al. 2013).

## 1.3 Approach

The information found in the literature generally suggests that reef-effect around wind farms:

- has a short spatial range (<100m)

- is species specific
- varies with season and time of the day

Given the above, an approach able to sample across different times of the day and for a longer period was deemed appropriate. For this, an automated and remotely piloted platform was chosen, the Sailbuoy (Offshore Sensing). This platform can be manually piloted as well as set on autopilot, allowing for continuous operation throughout the entire sampling campaign.

A distance gradient sampling design was preferred with respect to a control vs. effect design, to account for the large spatial and temporal variability of the system and having little information beforehand to appropriately choose a relevant control area.

To investigate fish aggregation patterns, echosounder technology was used, with sensors specifications able to monitor the entire water column in the area (max 120m depth).

The current preliminary study was not aimed at looking at seasonal differences, therefore the 4-weeks sampling effort required by the customer was concentrated in the same season (summer).

## 2 Material & Methods

---

### 2.1 Selected technology

Data on fish distribution in the wind park area were collected by means of active acoustic by surface glider platform, the Sailbuoy (by Offshore Sensing).

#### 2.1.1 Platform

The Sailbuoy is a small autonomous sailboat (length = 2m, weight = 60kg) with no propeller, using wind for propulsion and solar energy to power the onboard instrumentation (<http://www.sailbuoy.no/>, see Figure 1). The following instruments were loaded onboard the Sailbuoy: a GPS and satellite connection for location and data/commands transfer, temperature, salinity, oxygen and frequency fluorescence sensors for oceanographic and biological parameters.

#### 2.1.2 Sensors

A downward looking echosounder, SIMRAD WBT mini EK80 (<https://www.kongsberg.com/fr/maritime/products/ocean-science/fishery-research/echosondeurs-scientifiques/simrad-wbt-mini/>), mounted with a 200 kHz transducer, was used to measure backscatter and monitor the presence of fish in the water column down to the bottom (about 100 m deep). The echosounder was gimbed in the roll direction of the glider (fixed on the pitch).

Sensors for water temperature and conductivity (NBOSI), oxygen saturation (Optode 4835, Anderaa), and Chla fluorescence and optical backscatter at 700 nm wave length (EcoTriplet, SeaBird Scientific) were also installed on the Sailbuoy.

#### 2.1.3 Sensors' settings

Oceanographic data and fluorescence were sampled every 15 minutes, while echosounder data were sampled differently depending on the distance to the park. When actively passing through the park and slightly before entering the area, the echosounder was turned on to measure for 10 min every 15 min, while when outside the wind park area it was set to sample every hour for reference.

Echosounder data were recorded in wideband (FM) mode for a frequency bandwidth of 185-255 kHz. Data were recorded to 200m depth with 33729 data points per ping (0.59cm sample thickness), 150W power and 2048 millisec pulse duration. GPS fixes were recorded just before and just after the first and last pings of each sample period.



*Figure 1 Deployment of the Sailbuoy outside of Bergen by Offshore Sensing and Redningselskapet*

## **2.2 Sampling campaign**

The Sailbuoy was deployed on June 8<sup>th</sup> 2021 from outside of Bergen (NO) by Offshore Sensing with the help of Redningselskapet (Figure 1) and sailed to Hywind (UK) in 14 days. Low winds did not allow active crossings of the park until June 25<sup>th</sup>, which was the first day of sampling on site. Data sampling lasted 4 weeks, and on July 23<sup>rd</sup> the Sailbuoy started its return trip to Bergen. The return trip lasted 24 days and the Sailbuoy was collected outside of Bergen on August 15<sup>th</sup> (Figure 2, Figure 3).

During the data sampling period (June 25<sup>th</sup> to July 23<sup>rd</sup>), 15 days were spent around or outside the park, due to low winds, while active piloting through the wind farm was possible during 13 days. On those days, 17 active passes were done (1 to 2 per day, Figure 4).

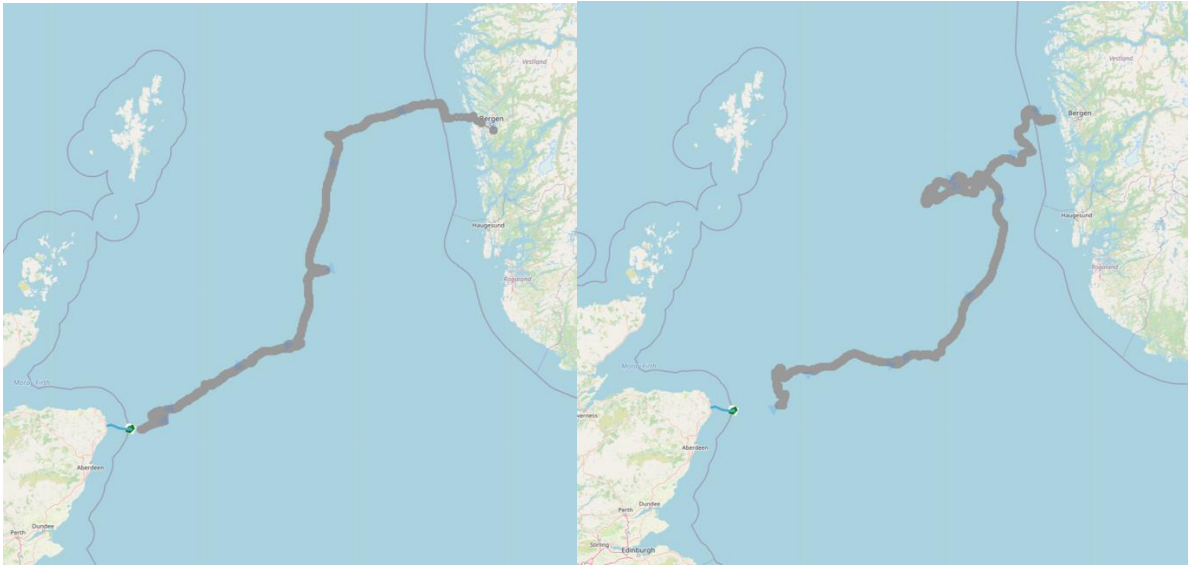


*Figure 2 Sailbuoy route from Bergen to Hywind (left, 15 days) and return (right, 24 days). The longer duration of the return trip was due to unfavourable winds that did not allow for a straight route.*



*Figure 3 Retrieval of the Sailbuoy by Redningsselskapet.*



Figure 4 Sampling tracks on site (June 25<sup>th</sup> to July 23<sup>rd</sup>). Grey dots are GPS positions, blue dots represent EK80 samples, every 15 min and every hour respectively within and outside of the operation area (white rectangle).

## 2.3 Sampling area and risk mitigation

An area of operation of about 8x4 km around the park was agreed with Equinor (Figure 5), based on the expectations from literature research of a relatively small-scale reef-effect (in the range of hundreds of meters). Transect lines in the form of distance gradients to the park, from min 1 km distance, with no predefined direction, were chosen as the sampling design to reach the scientific goals while mitigating the operational challenges (shifting currents due to tidal flow). Note that data sampling was intermittent and not continuous on all transects (see below 2.1.3).

Mission planning was performed by identifying risks and identifying mitigation solution. Due to the challenging piloting conditions in and around the operation area, the time and direction of the active crossings through the park were planned based on the timing and direction of the tidal current (sailing with the current). A maximum of two transects in opposite directions were possible during one day, with about 6 h difference.

When active sailing was not possible, the Sailbuoy was parked at a distance from the installations to avoid risk of collision and entanglement. The same parking area was used repetitively and can therefore be used as a control site in addition to monitoring a distance gradient.

Ship traffic density is high outside Peterhead, however low in a restricted area around the wind park. This area was chosen beforehand to park the Sailbuoy when not actively sailing. When on site, the area turned out to be too small (currents were stronger than expected and winds often low), and a different parking area was identified 12-15 km east of the park, as the risk of collision with the installation when parked was deemed higher than with other vessels in a trafficked area.

A visualization portal, Blue Insight by Kongsberg Maritime (<https://www.kongsberg.com/no/maritime/products/ocean-science/blue-insight/>), was used to visualize the position of the glider in real time with respect to the wind farm installations as well as other objects of reference (boats with AIS passing within 1nm of the glider,

bathymetry, coastline, etc). This was instrumental in mission planning, mitigating risks and in conducting the survey.

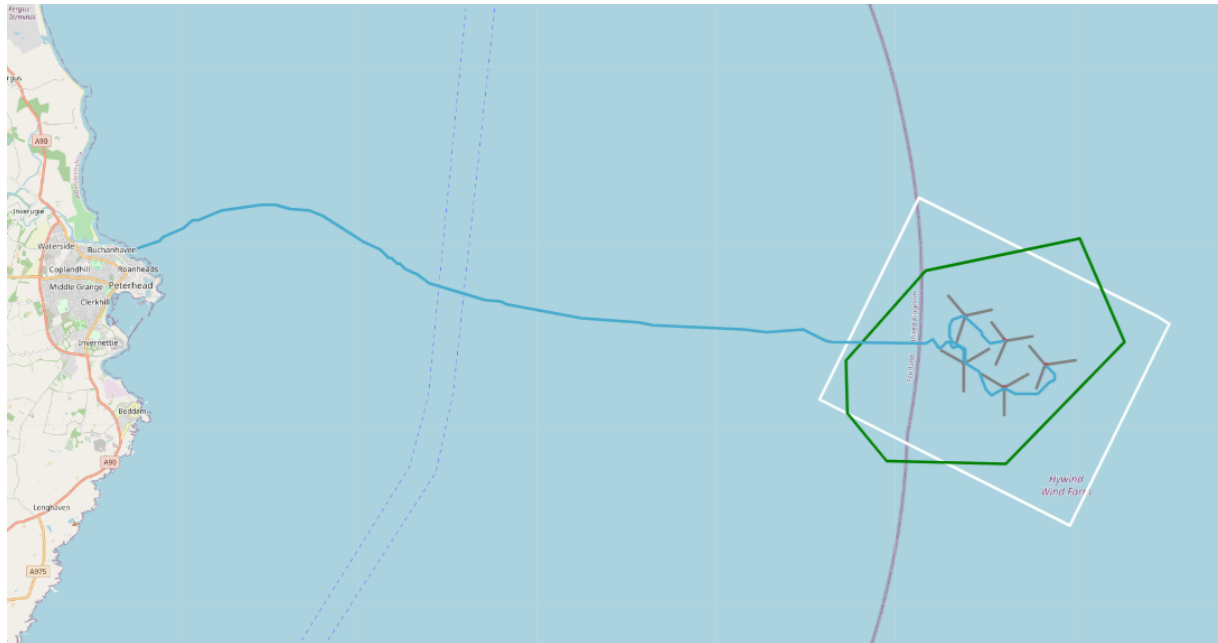


Figure 5 Hywind Scotland offshore wind park, with 5 turbines (anchor lines in grey, connecting cables in blue) outside of Peterhead (UK). The area of operation (about 8x4 km, white rectangle) and a restricted area of low marine traffic (green polygon) surround the installations.

## 2.4 Data analysis

### 2.4.1 Echo sounder data analysis approach

The raw echosounder data (backscatter in dB) were first analysed by Echoview® (Echoview Software Pty Ltd, Hobart, Australia) to:

- remove signal background noise (i.e. surface air bubbles, seafloor)
- identify fish schools vs other things (e.g., zooplankton layer/aggregations or infrastructure parts). It is possible that in some recordings the floating chains of the turbines are visible
- characterize fish schools (height and width, or area) and its average signal strength

All echosounder pings (and therefore any metrics based on position, distance or speed) are referenced to interpolated locations assuming a constant platform direction and speed.

A subset of 5 samples were used to develop a workflow in Echoview, which was subsequently applied to the full suite of data. Subjective decisions were made within the workflow, in particular dB thresholds for object detection and analysis, minimum school sizes, and target detection parameters. However, the automated process ensures that once these decisions have been made, the same (subjective) values are consistently applied across the entire data set.

The following workflow was applied:

1. Clean: Identify and mitigate background noise, intermittent noise, missing data, and other unwanted components of the data (i.e. surface, bottom and non-biological signal).
2. Detect: Define the bottom depth, detect volume targets such as aggregations and point targets such as individual fish, and partition data.
3. Classify: Perform absolute and/or probabilistic classifications to differentiate and categorize detected targets.
4. Characterize: Calculate and report metrics from calibrated, cleaned and classified echograms, typically to describe distribution, density, abundance, biomass, and acoustic properties.

In this work, non-calibrated data were used, as these only need to be compared relatively to each other. Data calibration will be performed at a later stage for scientific publication, in order to make the study comparable to others.

### 2.4.2 Noise removal

A surface exclusion line (above which data were considered surface noise) was typically identified below 1m depth (and more than 10 m depth in places). A bottom exclusion line was calculated using smoothing algorithms and a vertical threshold of 1.5m was applied in addition, to ensure all bottom related signal was excluded from further analysis (Figure 6).

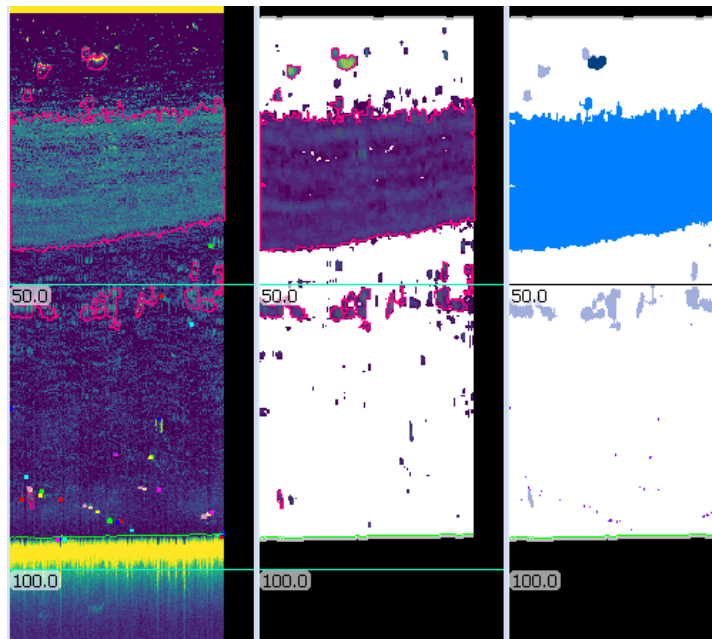


*Figure 6 Example sample period. From left to right: raw pulse compressed wideband Sv variable, processed echogram after cleaning and image processing, colour-coded-by-regions echogram. Pink outlines are school region borders and the smaller multi-coloured outlines closer to the bottom in the first two echograms are tracked target regions.*

In a few instances, a strong reflection signal was attributed to non-biological matter and cross matched with the positions of the Sailbuoy. The non-biological signal was isolated and removed from further analysis.

### 2.4.3 Biomass detection and classification

- a. Echoview's school detection algorithm was used to automatically delineate volume targets of interest as school regions (including both fish and zooplankton, pink lines in Figure 6). The following classes were identified:
  - layers (which aims to capture the diel vertical migration (DVM) component of the backscatter, needs to be min 2 m high to be classified as such),
  - strong schools within layers (indicating a strong fish school within the migrating layer or a large aggregation of zooplankton within the zooplankton layer itself),
  - strong schools outside layers (likely dense fish schools), and
  - weaker schools (which may include less dense aggregations of fish and/or smaller portions of the DVM component).
- b. Echoview's single target detection operator was used to automatically identify point targets (such as individual fish) based on a localised peak in signal strength.

Processed echograms, with data points color-coded based on classified regions, were exported to PNG files. A custom colour scheme was created in Echoview for this (Figure 7).

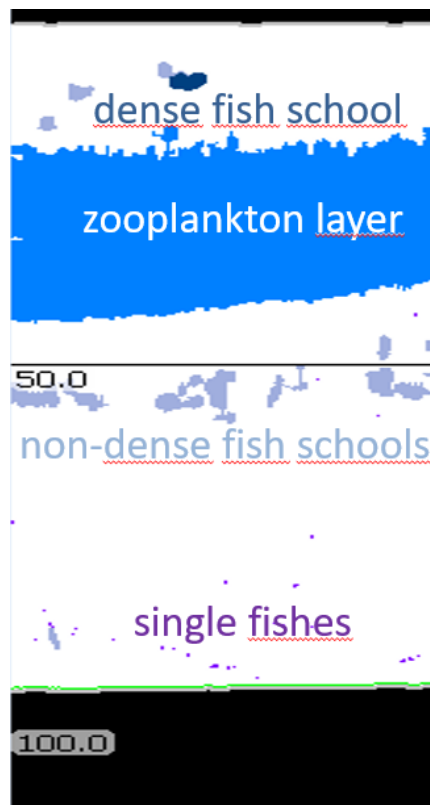


Figure 7 Classification of detections. Medium blue = main migrating layer (zooplankton), Dark blue = particularly strong backscatter within the main migrating layer (dense fish schools or aggregated zooplankton, not shown in picture), Navy blue = particularly strong backscatter independent of the main migrating layer (likely dense fish schools), Light grey/blue = weaker backscatter independent of (or smaller in length than) the main migrating layer (likely non dense fish schools or part of the migrating layer), Purple = targets (likely individual fish).

#### 2.4.4 Choice of indicators

Different variables were used to characterize fish and zooplankton biomass and aggregation characteristics, depending if single targets or schools were detected. For schools (or zooplankton layers), the total backscatter for a school (area backscattering coefficient, ABC, also called  $S_a$ , units  $m^2m^{-2}$ ) was used as a proxy of the school's biomass (McLennan et al, 2002). ABC for schools in the same biomass type (zooplankton, weak and strong fish schools) was summed for a 10 min sample, providing an estimate of total biomass per type per sample integrated for the entire water column. Volume back scatter,  $S_v$  (in dB ref  $m^2/m^3$ ) was used as a measure of biomass density (per  $m^3$ ) and presented as the average  $S_v$  per 10 min sample per biomass type.

For single fish targets, target density (the number of targets standardized by the water volume sampled, unit count/ $m^3$ ) was used as an index of abundance density.

### 2.5 Distance gradient from the park

To investigate the potential of reef-effect of the installations, different distance measures were calculated between the installations and each of the echosounder samples. The closest distance between a sample and any of the 5 turbine bodies or anchoring chains was calculated to look at the small-scale effect of infrastructure on abundance. To look at a broader effect of the park as a whole, the distance of each sample from the middle of the park was used.

In addition, we divided the samples into the following categories, which represent different distance classes, but may also give an indication on the level of human disturbance in the area (see 2.6.1):

1. Near Installations: samples within 100 m from a turbine body or anchoring chain (light blue area in Figure 8).
2. In Park: samples within the park, defined as an area around the 5 turbines with a 500 m buffer zone (dark blue area Figure 8)
3. Low Traffic area: samples outside the park, but within an identified area of low traffic (visually done via Marine Traffic annual statistics maps, light grey area Figure 8)
4. Outside: samples outside the aforementioned areas

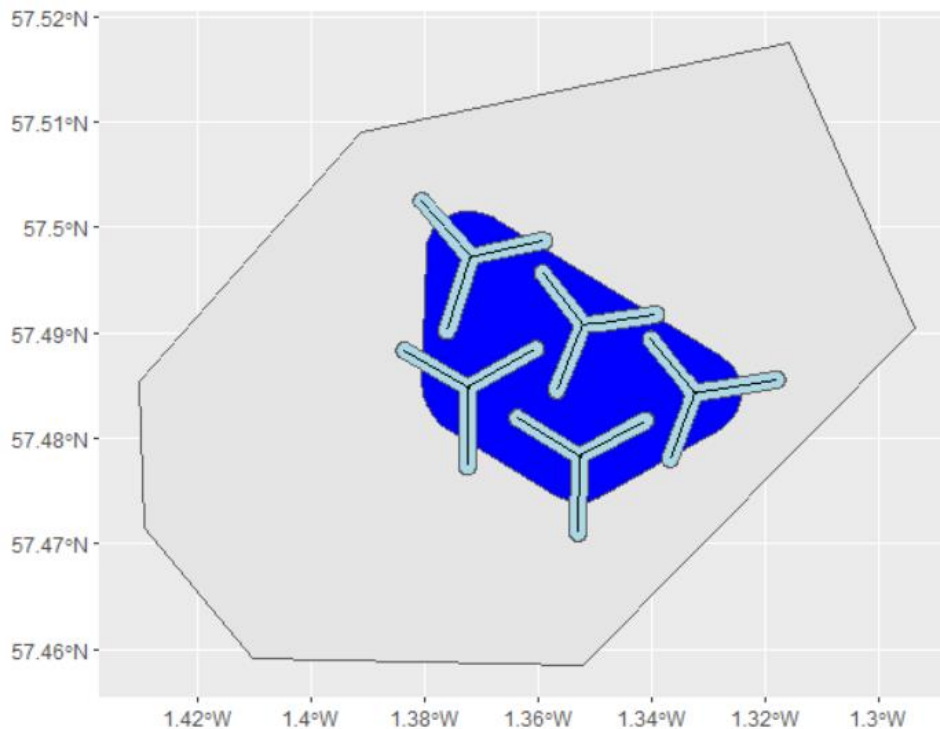


Figure 8 The different areas used to categorize distance from the installations and level of traffic/fishing pressure. 1) A "near installation" area was defined as the area within 100 m of any installation (turbine body or anchoring chain, light blue), 2) the park area was defined as the area within the perimeter of the 5 turbine bodies (with a buffer of 500 m, dark blue), 3) a "low traffic" area was visually identified from Marine Traffic (light grey here, corresponding to dark blue area in Figure 9).

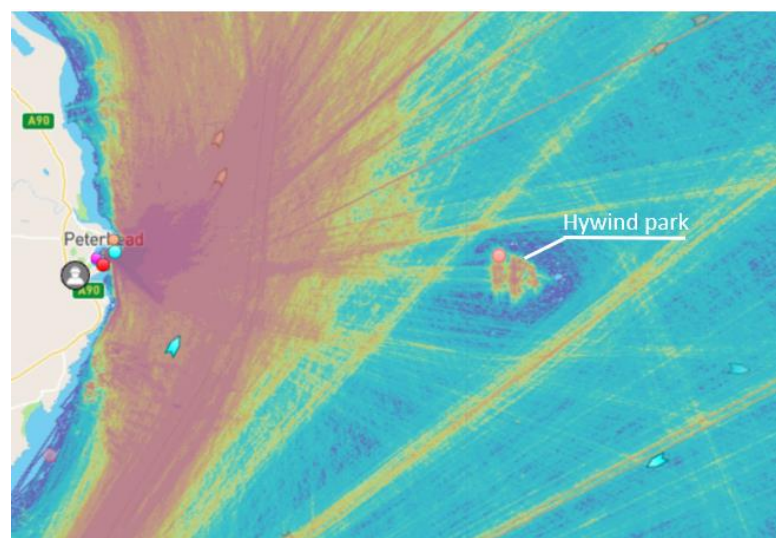


Figure 9 Screenshot from Marine Traffic of 1 year traffic data in the area around Hywind Scotland. The area outside of Peterhead is characterized by high vessel traffic (all vessel types, increasing from yellow to red), as well as the area between the turbines, due to vessels servicing the park. A low traffic area with little traffic (dark blue) is seen around the wind park, probably as a consequence of vessels avoiding the park.

## 2.6 Environmental and human factors

### 2.6.1 Marine traffic and fisheries

Accurate data on marine traffic and fisheries are likely available, but time consuming to acquire and this analysis was not within the scope of this project. We however thought it relevant to include a rough proxy for these two types of disturbance. Fisheries and traffic are likely spatially diverse and do not display gradual change proportional to distance from the park. The distance categories outlined in 2.5 were therefore used to simplify the complex relationship between 1) potential attraction to the farm for nutrients and protection from predators and fisheries, and 2) potential avoidance of areas with intense traffic (causing noise disturbance). The distance classes were likely characterized by the different degrees of traffic and fisheries in the following manner:

Area	Traffic	Fisheries
1. Near Installations	medium to high	low
2. In Park	high	low
3. Low Traffic area	low	likely low
4. Outside	high	high

### 2.6.2 Bottom depth and light regime

Bottom depth was identified per sample as the average of the bottom detection per ping in each sample (see analysis from Echoview in Methods 2.4.1). Each sample was classified into a day or night category, based on the average time for dawn and dusk at Peterhead during the one-month sampling campaign: dawn 4:00 am, dusk 22:00.

## 2.7 Statistical analysis and spatial interpolation

Temporal and distance trends in the different measures of biomass/abundance are presented as loess smoothers of the points. Spatial interpolation, to obtain distribution maps, was done by kriging of the logged biomass index values (ABC) on a spatial grid of 1 km<sup>2</sup> cells. An exponential spatial correlation variogram model was used and a maximum extrapolation distance of 2 km (i.e. the data in one echogram would not predict further than two cells away).

# 3 Results & Discussion

---

## 3.1 Interpretation of figures

Due to the complexity of the data and the large variability of results between different taxonomic groups, times of the day, bottom depths, etc, the results in this report are often presented in plots with multiple panels (plot sections), which show the same information (x and y axis) for different subsets of the data for comparative purposes.

Figure 10 describes how to interpret a generic multiple-panels plot, which uses two variables (one numeric and one categorical, top and right grey labels) to subset the data. Since each variable has in this case two intervals or classes the plot has 2x2 panels with shared x and y axes (bottom and left black labels). The subset of data within each panel is shown in the panel title (dark grey rectangle). Continuous variables (eg. depth, time) are split into intervals for subsetting purposes. Brackets around intervals indicate if the interval includes " [" or does not include "(" the intervals' extremes.

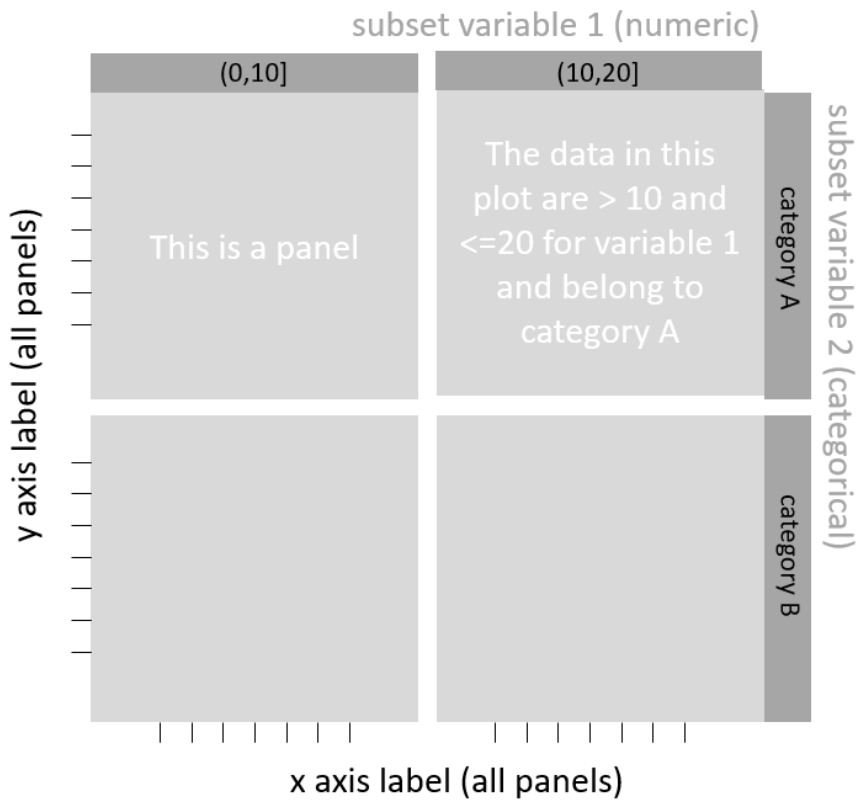


Figure 10 A generic multiple-panel plot and how to interpret its content.

## 3.2 Data sampled

A total of 241 echosounder samples (10 min continuous recording) were taken within the area of operation (white box in Figure 5 and Figure 3), and 710 outside of it. With approximately 10 min per sample, a total of 40 and 118 hours of acoustic backscatter data were sampled respectively in and outside of the area of operation (total = 158 h).

Due to logistical challenges in keeping the platform within the predefined area of operation (i.e. low wind and high currents), the echograms sampled during the campaign ranged from a min distance of 150 m to a maximum distance of 35 km from the turbines Figure 11. Most of the active transects (sampling in the area of operation) were done in the afternoon, but a certain amount of samples were also taken during morning and evening, very few samples were taken between midnight and 4 am (Figure 12).

Two of the samples recorded near the installations included a probable anchoring chain detection in the backscatter signal (26 June at 09:24, see Figure 13, 7 July between 11:18 and 11:22).

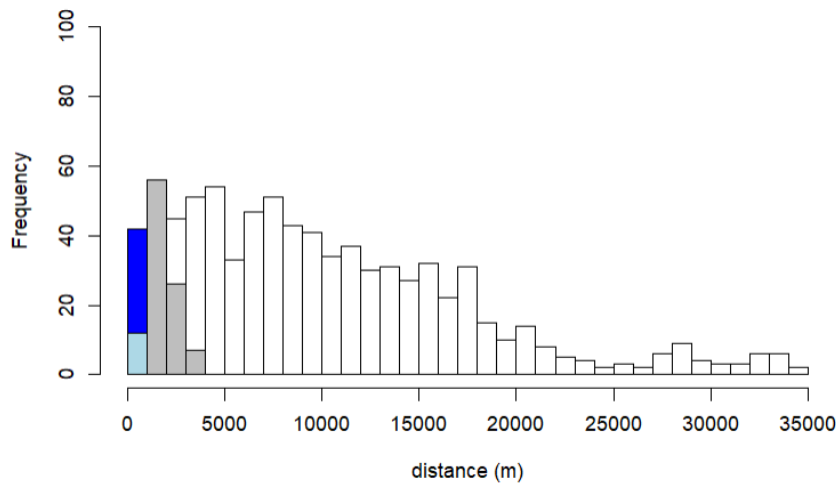


Figure 11 Frequency of the distances of echosounder samples from the infrastructure. The colours represent the samples taken in the different distance categories from the installations (see Figure 8 for colour reference).

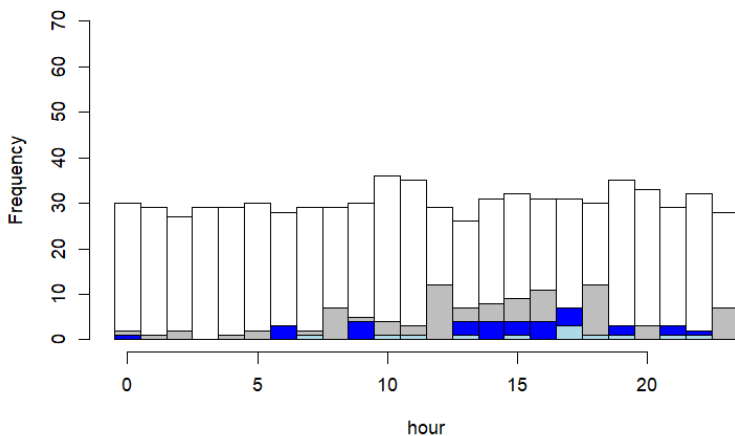


Figure 12 Frequency of data samples per hour of the day. The colours represent the samples taken in the different distance categories from the installations (see Figure 8 for colour reference).

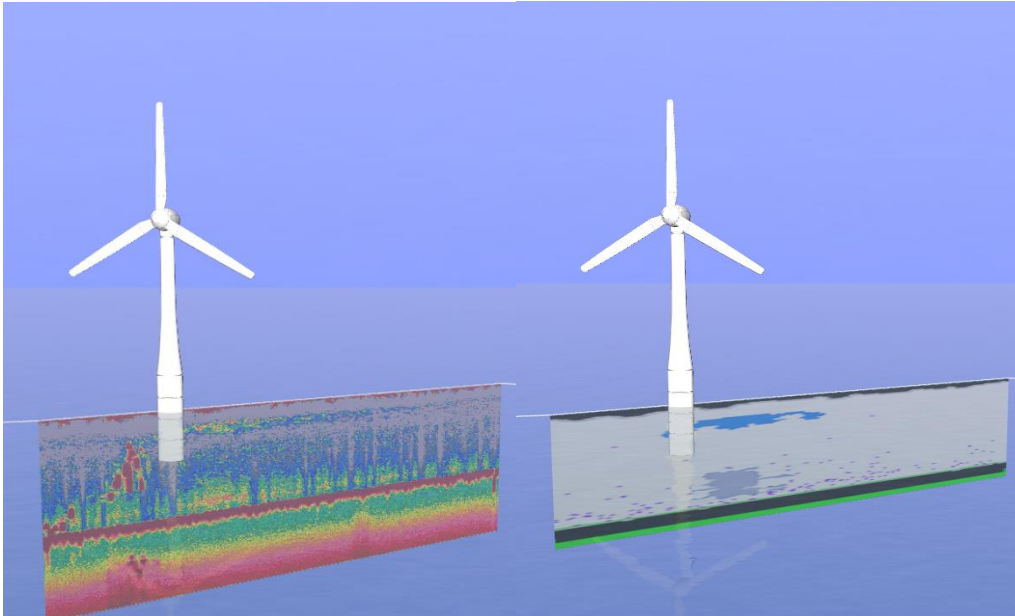


Figure 13 Screenshot from Blue Insight for the echogram of June 26<sup>th</sup>, showing the anchoring chain (dark red, left), removed in the analysed echogram output (right).

### 3.3 Effect of environmental factors on fish biomass, density and vertical migration

#### 3.3.1 Bottom depth

The bottom depth of the samples collected within the park area and in the low traffic area ranged between 100 and 120 m, while a much broader bottom depth range characterized the samples outside of this area (as shallow as 60 m, Figure 14). However, depths within 8 km distance from the park had a comparable range across all distance categories.

An increasing trend in the overall biomass of zooplankton (Figure 15 A, top panel) and in the density of single fish targets (Figure 15 C) was found for areas with deeper bottom, while this trend was not apparent for schooling fish. It has to be noted that the ABC (area backscatter coefficient) is a measure of backscatter integrated throughout the water column, so ABC in deeper areas is integrated over a larger water volume than shallower areas. Sv (volume backscatter) however is proportional to the density of a school or layer per m<sup>3</sup> of water and this index also showed a slight increase with bottom depth (Figure 15 B).

An increasing biomass trend with bottom depth does not necessarily mean that the higher biomasses are located at depth. When looking at the biomass location in the water column (biomass depth), schools and layers showed varied patterns of total biomass. Despite the variety of the patterns, total biomass often peaked at mid depths and decreased in deeper waters (Appendix Figure 29 A) suggesting that biomass is not higher at depth. For single targets density seemed to peak at an average of 90 m depth, but not at its deepest (Appendix Figure 29 B).

We can therefore conclude that the higher biomasses in areas with deeper bottom are either due to the higher water column (larger amount of space between surface and bottom to host fauna) and/or to a generally higher productivity of deeper areas (Buchan deep).

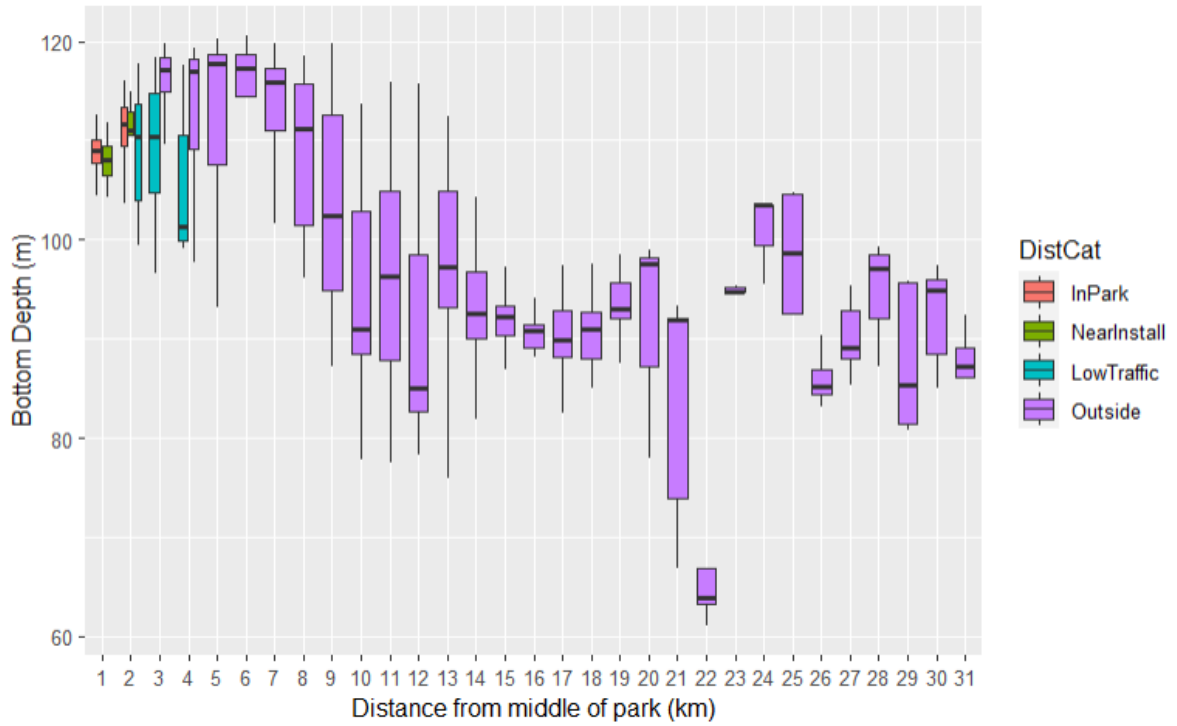


Figure 14 Bottom depth (y axis) of all echosounder samples based on their distance from the centre of the park (x axis) and the minimum distance from any installation (colour scale category).

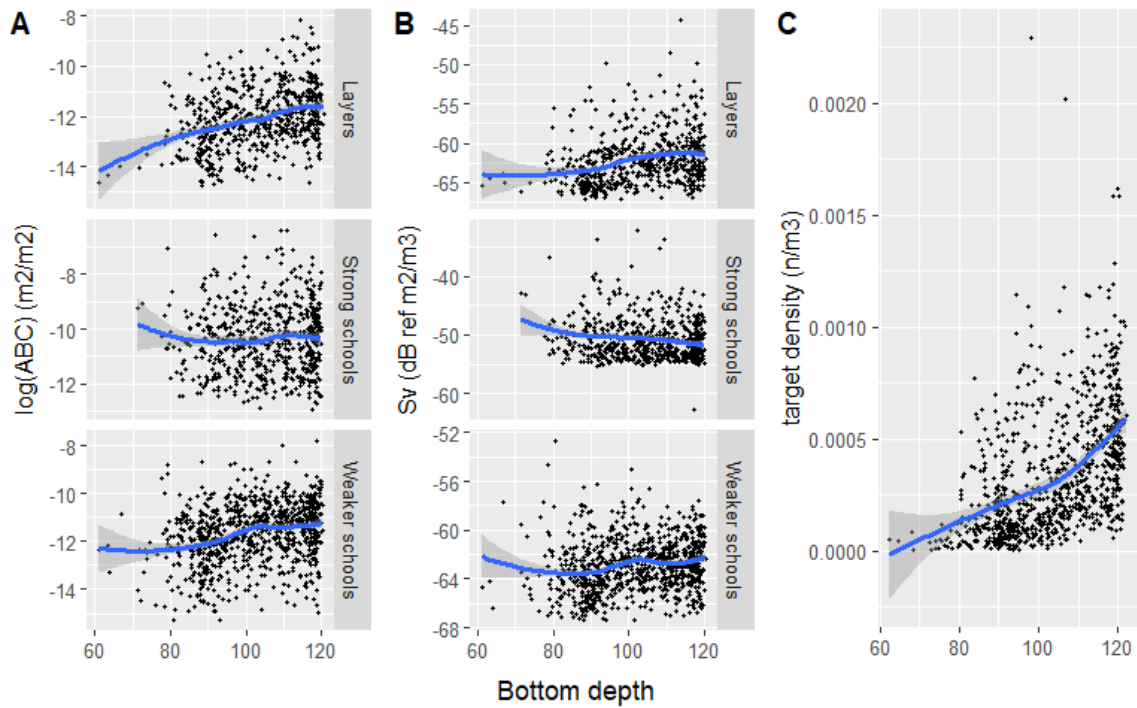


Figure 15 The total biomass per 10 min sample of fish schools and zooplankton layers ( $\log(ABC)$ , A), its biomass density ( $S_v$ , B) and the density of single fish targets (C). Zooplankton biomass (A top panel) and single fish density (C) increased with the sample's bottom depth (x axis). See 2.4.4 for specifications on ABC,  $S_v$  and target density. All depths are shown in meters.

In the particular case of single fish target density, its increasing trends with the sample's bottom depth, however, could also be caused by the intrinsic higher detectability of the echosounder with depth. In fact, the detectability of a physical target, by an echosounder placed at surface, increases with depth due to the conic shape of the acoustic beam. Being the beam wider with depth implies that the volume of water sampled is higher at higher depths, with a consequent higher likelihood to detect a target (Figure 16).

A positive relationship between bottom depth and single fish density was found in this study. To understand if this was likely to be caused by an increased detectability with depth, the data should be further analysed and compared within depth bins rather than using variables characterizing the entire water column. In case of a detectability issue, fish density should be constant within a determined depth bin across samples with different bottom depths. This analysis was outside the scope of the present study, but is suggested for further scientific publication of the results.

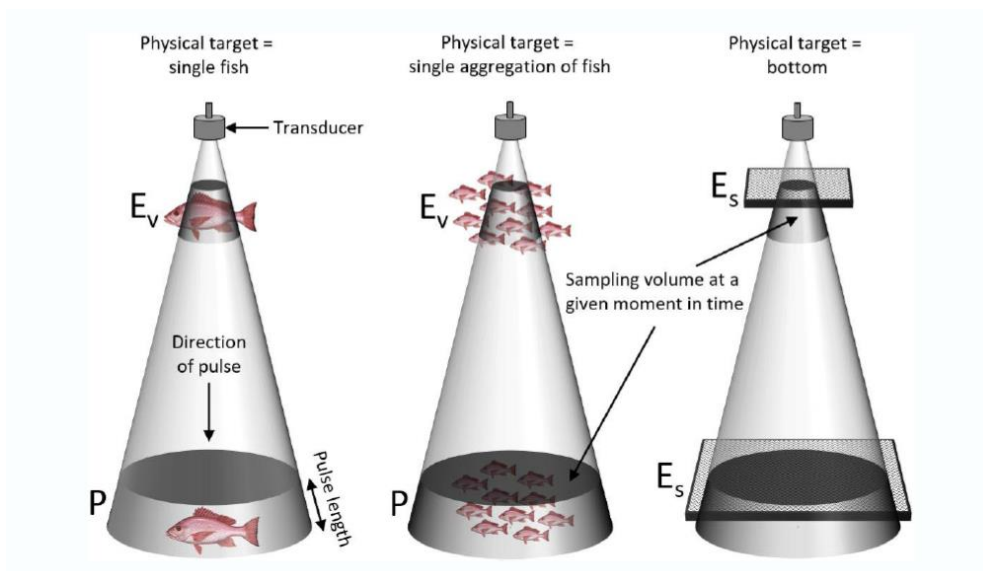


Figure 16 The detectability of a physical target increases with depth due to the conic shape of the acoustic beam, which samples higher volumes of water at higher depths (courtesy of Echoview Software Pty Ltd).

### Summary:

The sample's bottom depth had a positive effect on the estimates of zooplankton layers' biomasses and single fish densities, but not on fish schools' biomasses. Given the wide range of depths sampled on the distance gradient from the park, comparisons of biomasses at different distance to the park should be done within similar bottom depth classes or alternatively within 8 km from the park.

### 3.3.2 Diel vertical migration

Fish schools, as well as zooplankton layers, were generally found to migrate from surface to depth at dusk and reverse the pattern at dawn (Figure 17). Diel vertical migration (DVM) is a well-known and documented phenomenon. DVM patterns have been previously shown in cod (*Gadus morhua*) and whiting (*Merlangius merlangus*) inside and around an offshore wind farm at Horns Rev off the coast of Danmark (Leonhard et al. 2013). The reason for this migration is assumed to be a trade-off between preying on lower trophic levels at surface at night and avoiding visual predators at daylight. Part of the zooplankton and fish schools, however, did not perform any vertical migration at all, remaining at surface all day long. This is likely a consequence of schools and layers being a mixture of different species, and of vertical movement behaviour being species specific. On the other hand, sandeels (*Ammodytidae* spp.), a characteristic species in the North Sea, are known to conduct reversed DVM patterns, being found in the upper water column in daytime and buried in the sand in night-time (e.g., Leonhard et al. 2013).

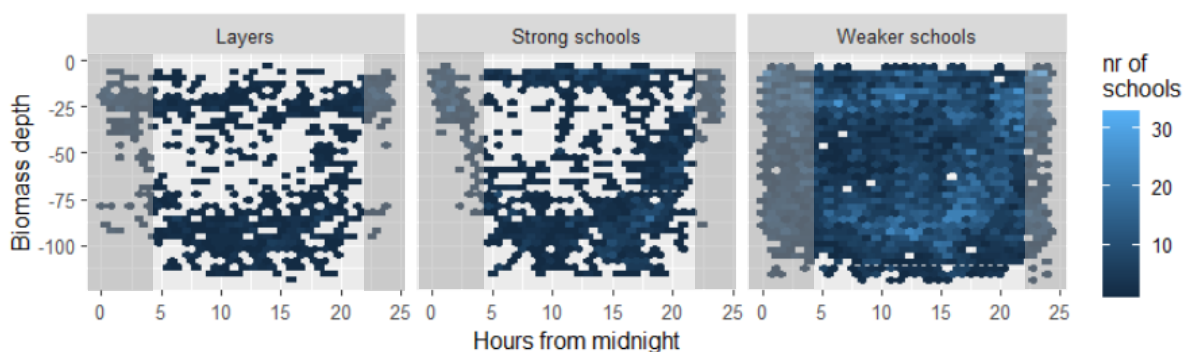


Figure 17 Nr of identified zooplankton layers or fish schools (colour scale, see legend) for a specific depth (y axis) at time of the day (x axis). The hours of the day before dawn and after dusk are shaded.

Visual inspection of the DVM patterns in this study showed generally mirroring patterns around noon, hence some of the results presented in this and further sections are shown by "hours difference from/to noon" for 4 categories: 0-3, 3-6, 6-9 and 9-12 h. Due to the lower sampling frequency in the park area during night and early morning (see Figure 12), however, care should be taken in concluding on the occurrence of specific patterns within the park area for these time periods.

In this dataset, the extent to which the biomass at surface was migrating towards the bottom depended on bottom depth and school type (Figure 18). Schools in deeper areas showed larger migration ranges, which can be a consequence of migrating all the way to the bottom, rather than to a fixed maximum depth. Dense fish schools performed larger migration ranges than non-dense schools (usually found at mid water depth, Appendix Figure 30). The reason for this difference can be because dense schools may split up in smaller and less dense patches during the vertical migration, accounting for the increased number of non-dense schools at mid depth (in the middle of an upward or downward migration). The difference between school density categories can be due to different species compositions (with different backscatter signatures) or a different density of the same species. Further analysis aimed at species identification would be necessary to draw further conclusions on this topic.

In addition, the variation in vertical distribution of the different school types was much higher during daytime, when multiple frequency peaks were to be found at different depths (e.g. at

surface and at the bottom, Appendix Figure 30), both for fish and zooplankton. Dense fish schools at the surface were generally shallower than the fraction of zooplankton remaining in the upper water column, but extended slightly deeper and overlapped the main zooplankton layer, when this was gathered sub-surface at night (Appendix Figure 30). The occurrence of non-dense fish schools is higher at mid water depths during daytime, which suggests that the level of biomass aggregation at daytime is generally lower.

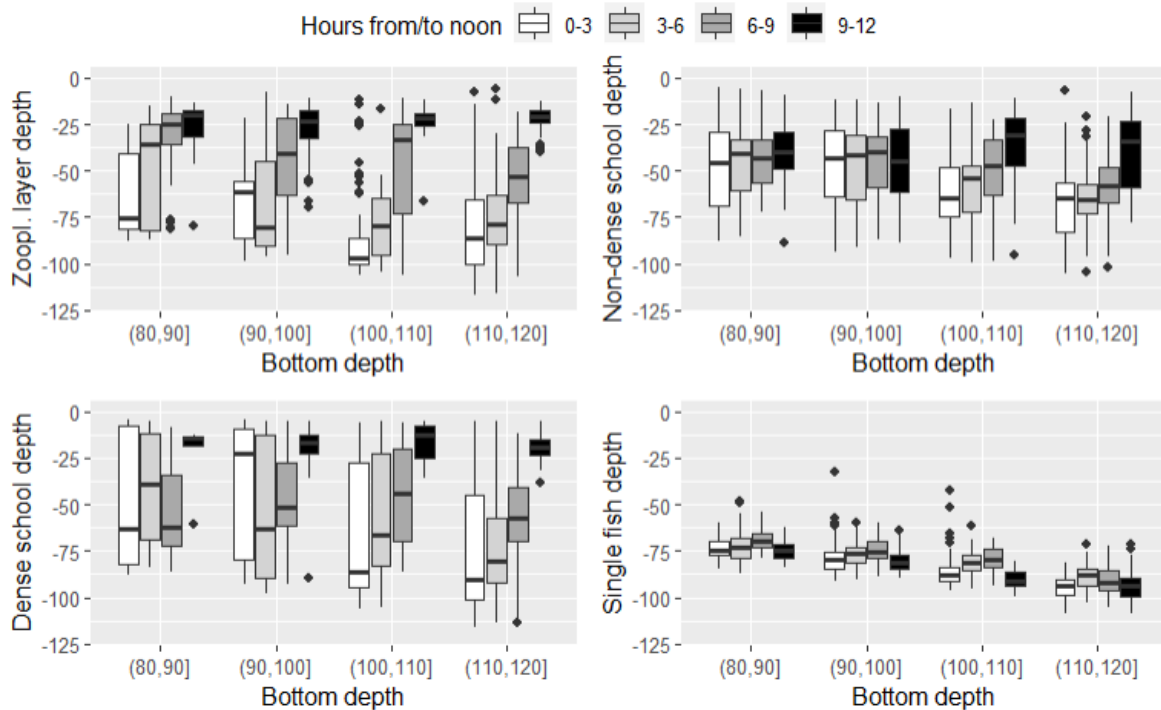


Figure 18 Vertical distribution (boxplot) for zooplankton, dense and non-dense fish schools, and single fishes for 4 times of the day (hours difference from/to noon 0-3h = from 9:00 – 12:00 & 12:00 – 15:00, 3-6h = 6:00 – 9:00 & 15:00 – 18:00, 6-9h = 3:00 – 6:00 & 18:00 – 21:00, 9-12h = 00:00 – 3:00 & 12:00 – 24:00) and 4 bottom depth categories (x axis). All depths are shown in meters.

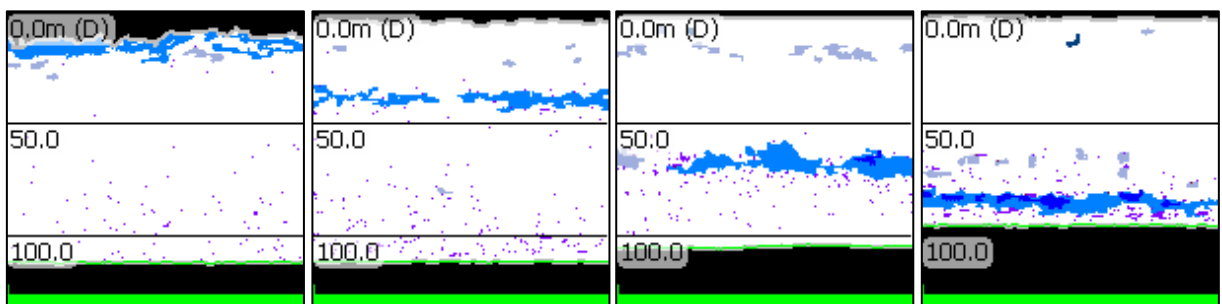


Figure 19 Analysed echosounder images for 4 samples (10 min each) on July 6<sup>th</sup> starting (from left to right) around 22:30h, 02:30h (next day), 04:30h and 06:30h. The figure shows the main migrating zooplankton layer (light blue) performing a DVM and moving toward the seafloor with the onset of day. Single fishes (purple dots) show a different pattern, with an upward migration towards the descending zooplankton layer, meeting it at intermediate depths and then descending with it towards the bottom. See Figure 7 for more info on analysed echograms and colour legend.

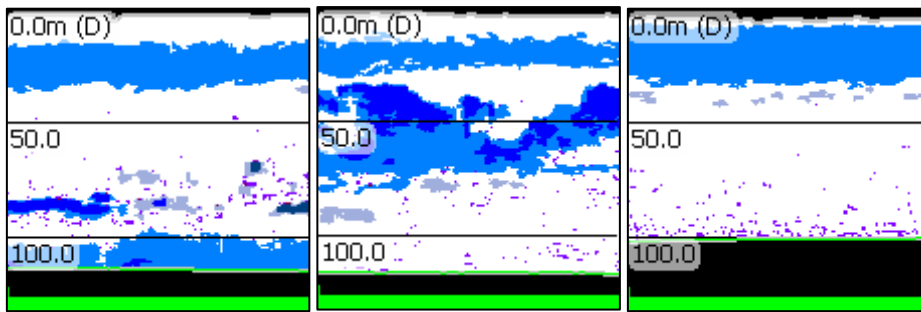


Figure 20 Analysed echosounder images for 3 samples (10 min each) on July 15<sup>th</sup> starting (from left to right) at around 18:00h, 20:00h and 22:00h. The figure shows how a fraction of the zooplankton layer (light blue) is migrating towards the surface during the evening (performing DVM), while another fraction did not perform any vertical migration. See Figure 7 for more info on analysed echograms and colour legend.

Migration patterns were found to be similar between zooplankton layers and fish schools (i.e. classical DVM pattern described above), but differ between fish schools and individual fish targets (Figure 18). Individual fish targets were found to be close to the sea floor at night, migrating upwards at dusk, then moving downward again after reaching a certain threshold depth, reaching maximum depth at noon, and reversing the pattern towards the evening (Figure 18).

This behaviour seems to be due to the attraction of single fishes, mostly bottom dwelling, to the main migrating zooplankton layer, likely for feeding, when the latter reaches middle to deep waters. This is shown in two series of echograms chosen as examples (Figure 19 and Figure 20).

Because of the contrasting direction of the vertical migration between fish schools and single fish targets, we can assume that the schooling fishes are likely different species (or age classes) than the individual targets. This is also supported by the average depth at which single targets occur, which is generally deeper than schooling fish (Figure 18). We can therefore exclude that the higher frequency of detection of single targets at depth, with respect to schools, is a consequence of the increased detectability of the echosounder (see 3.3.1).

DVM was found not to affect the overall biomass of schools, but had an effect on the density of single fishes per sample, with higher densities during night-time (Appendix Figure 31).

### Summary:

DVM highly affects the position of schools and single targets in the water column and showed the most complex spatial/temporal patterns in this dataset.

Fish schools and zooplankton performed a classical DVM from surface to bottom with the onset of day, while single fish targets had a more complex pattern and never reach the surface (likely different species than schooling fish).

DVM range changed with bottom depth, suggesting the aimed max depth of migration is relative to the bottom and not to the surface.

Aggregation was higher at night, when most of the biomasses were to be found towards the surface for schooling fish and zooplankton and the at the bottom for single fish targets.

A fraction of schooling fish and zooplankton did not perform DVM and was found at the surface all day (likely species and life-stage specific).

### 3.4 Spatial and temporal trends with distance to the infrastructures

#### 3.4.1 Oceanographic conditions and phytoplankton bloom

Monthly averaged water temperature and salinity profiles from the Buchan Deep (Figure 21) suggest the presence of stratification in the water masses generally between May and August, with a strong salinity gradient at about 20 m depth. In the 4 weeks of data sampling on site (mid-June to mid-July), surface temperature and salinity were steadily increasing (Figure 22), which is in line with the monthly averaged trends shown in Figure 21.

Despite the lack of temperature profiles during the field campaign, but considering the agreement between trends in climatological and sampled surface temperatures, we can assume that the climatological monthly profiles in Figure 21 are a good indication of the oceanographic conditions of the water column on site, and therefore that waters were stratified at the time of the data sampling.

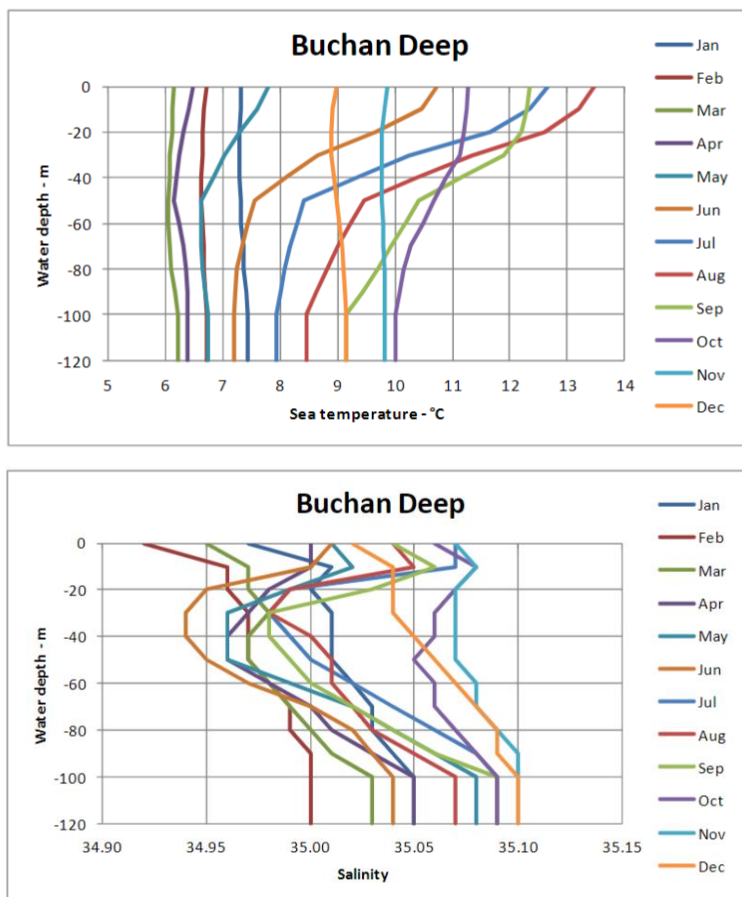


Figure 21 Monthly mean sea temperature and salinity profiles at Buchan Deep (source Hywind Buchan Deep Metocean Design Basis RE2014-002, data from World Ocean Atlas 2009 <https://www.ncei.noaa.gov/products/world-ocean-atlas>).

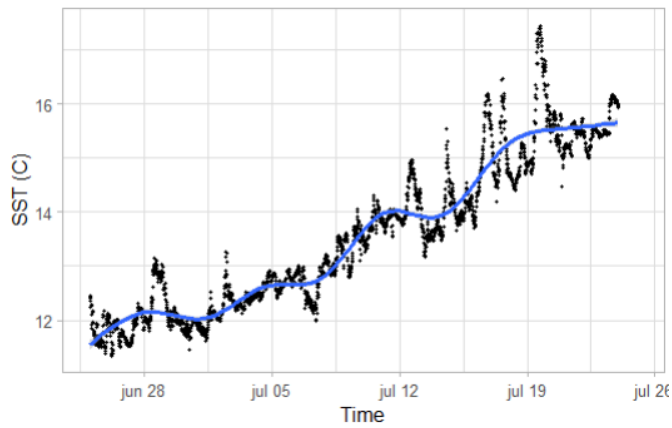


Figure 22 Sea surface temperature increasing trend measured by the Sailbuoy during the 4-weeks campaign. The peaks and lows are mainly due to day/night variation. Surface conductivity was highly correlated with temperature (0.99) and had the same increasing trend (not shown).

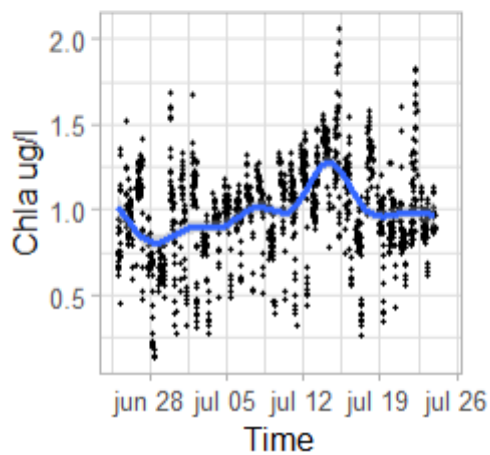
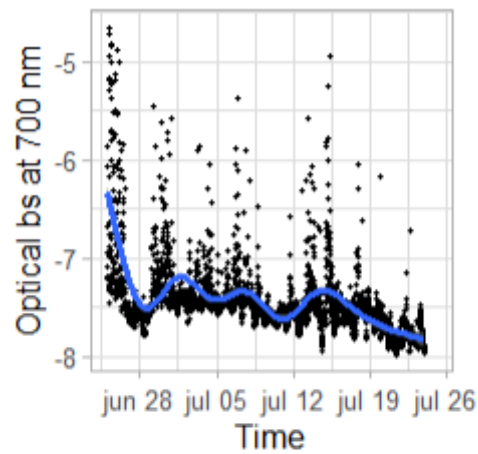


Figure 23 Temporal patterns of phytoplankton biomass indices, Chla carbon based on optical backscatter at 700 nm (top) and Chla concentration based on fluorescence (bottom).

The two indices of phytoplankton biomass (Chla concentration based on fluorescence, and phytoplankton carbon mass based on optical backscatter) showed similar patterns, with synchronous peaks and lows, but a different development in time. While Chla concentration seemed steady during the sampling period, carbon concentration progressively decreased during the 4 weeks, overall in the area.

The proportion between these two measures has been shown to vary during the year, based on the light and nutrient conditions, with the fraction of carbon to Chla concentration increasing in spring and decreasing towards autumn for open waters in the North Sea (Jakobsen et al 2016). In this study, despite some tops and lows, the overall trend was decreasing, suggesting that the sampling period was after the main peak of the bloom season in spring.

The Chla concentration index based on fluorescence is affected by daylight scattering at the surface (quenching). The data in Figure 23 has been filtered and only night-time (7pm - 7am) values are shown to avoid the bias.

### **3.4.2 Succession patterns**

The temporal patterns of zooplankton and strong fish schools were positively correlated (corr 0.5), particularly for larger zooplankton layers, while this was not true for zooplankton and weaker schools (corr -0.02, Appendix Figure 32). This suggests that increases in highly aggregated fish biomass corresponded in time and space with the increases in zooplankton biomass (Figure 24). When looking at the temporal patterns of the different biomass types, a succession pattern is evident, with phytoplankton concentration peaking earlier than zooplankton and fish biomass, and then decreasing when zooplankton and fish are at their maximum, likely as a consequence of grazing (Figure 25).

When looking at the data based on the distance from the wind park, the absolute values of the proxies for zooplankton and fish biomass were higher the closer to the park (different panels in Figure 25 & different smoothers in Appendix Figure 33), suggesting that secondary production, after a phytoplankton bloom, and the consequent aggregation response of fish, is higher in the vicinity of the park. The timing of the succession between primary and secondary producers seemed also somewhat shifted in time, depending on their distance from the park, with zooplankton and fish peaking during the second half of the sampling campaign close to the park (Figure 25).

The highest concentrations of zooplankton the study area differed in their spatial location from week to week (Figure 24), but the area of highest concentration overall was found to be south of the park during the 3<sup>rd</sup> week of sampling campaign. This is more evident when the biomass distribution maps are not in logarithmic form (Appendix Figure 35).

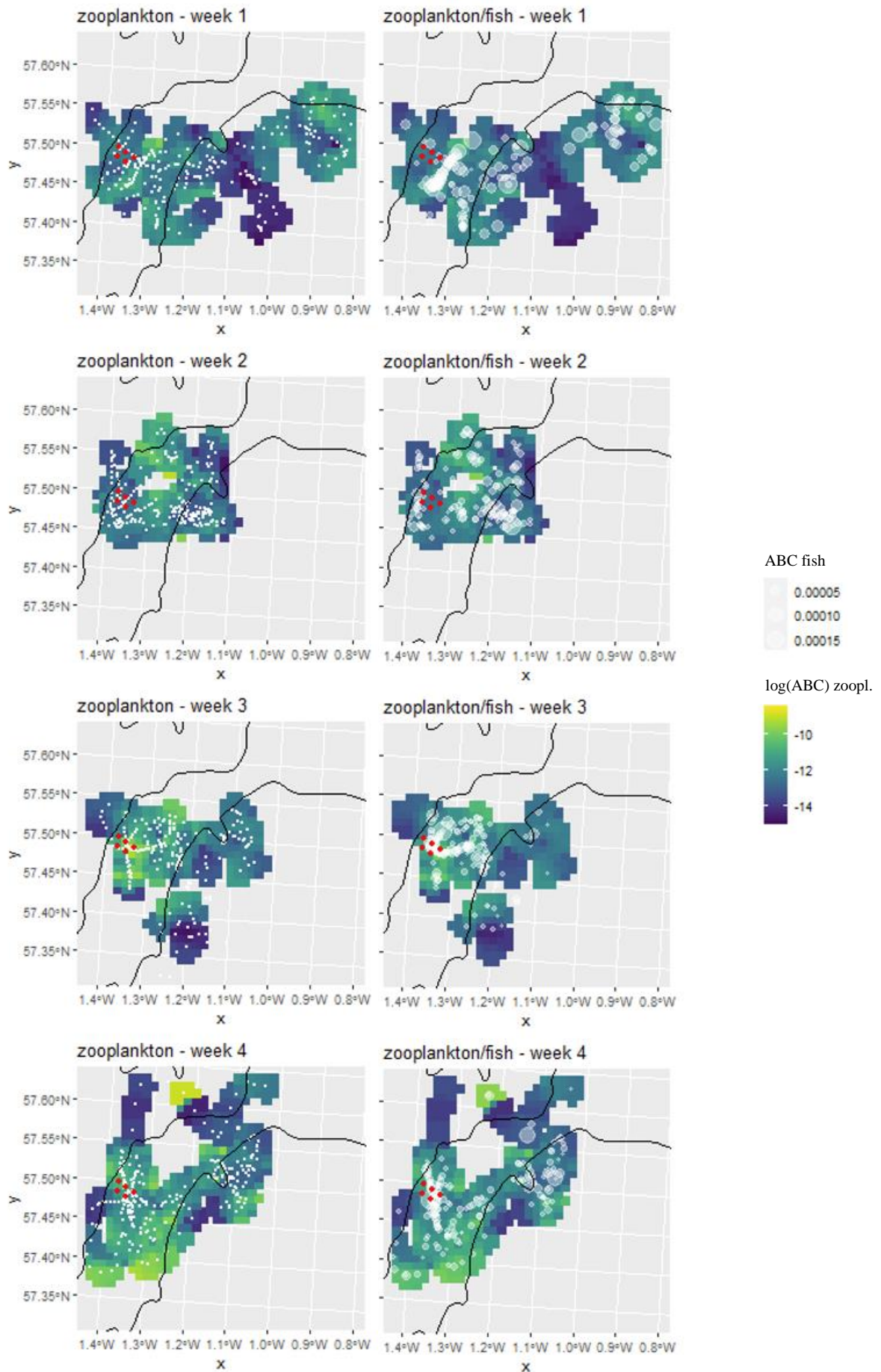


Figure 24 Weekly spatial distribution of zooplankton ( $\log(ABC)$ , colour scale, both columns plots) and strong fish schools ( $ABC$ , white bubbles superposed on right column plots). The zooplankton distribution maps are spatially interpolated (by kriging, see 2.7 for details) and the location of the data samples (echograms) are shown as white dots in the left column plots. The five wind turbines are marked as red dots in all maps, together with the 100m depth contour lines (black) indicating the location of the Buchan Deep corridor ( $>100\text{m}$ ).

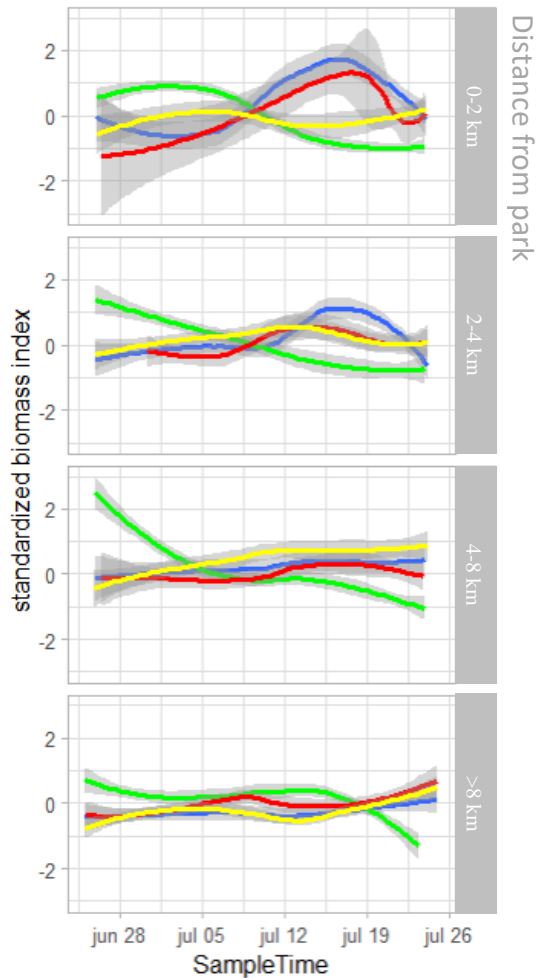


Figure 25 Comparison of trends in phytoplankton biomass (backscatter  $\text{m}^{-1} \text{Sr}^{-1}$  at 700 nm, green line), biomass ( $\log(ABC) \text{m}^2/\text{m}^2$ ) of zooplankton (blue line) and strong schools of fish (red line), and density ( $\text{nr}/\text{m}^3$ ) of single fish targets (yellow line). The lines are loess smoothers of indices with very different units, but these are all standardized to mean = 0 and sd = 1 for comparison of trends. Absolute values (e.g height of peaks) should not be compares across lines. The panels show the data collected between 0-2, 2-4, 4-8 and beyond 8 km from the centre of the park.

### 3.4.3 Effect of the distance from the park

Given the succession patterns described above, variation in a potential effect of the park with time was expected. Figure 26 shows the biomass indexes for zooplankton and schooling fish, together with the density of single fishes, on a distance gradient from the middle of the park. To exclude the effect of bottom depth on biomasses, as outlined in section 3.3.1, the samples were filtered to only include bottom depths > 100 m and limiting the distance gradient to 8 km from the centre of the park (see Figure 14). The plots confirm what was shown above, that the general increase in biomasses of zooplankton and highly aggregated fish schools in weeks 3 and 4 are higher the closer to the park. Weaker fish schools do not show any trend with distance, while single fishes show lower densities close to the park.

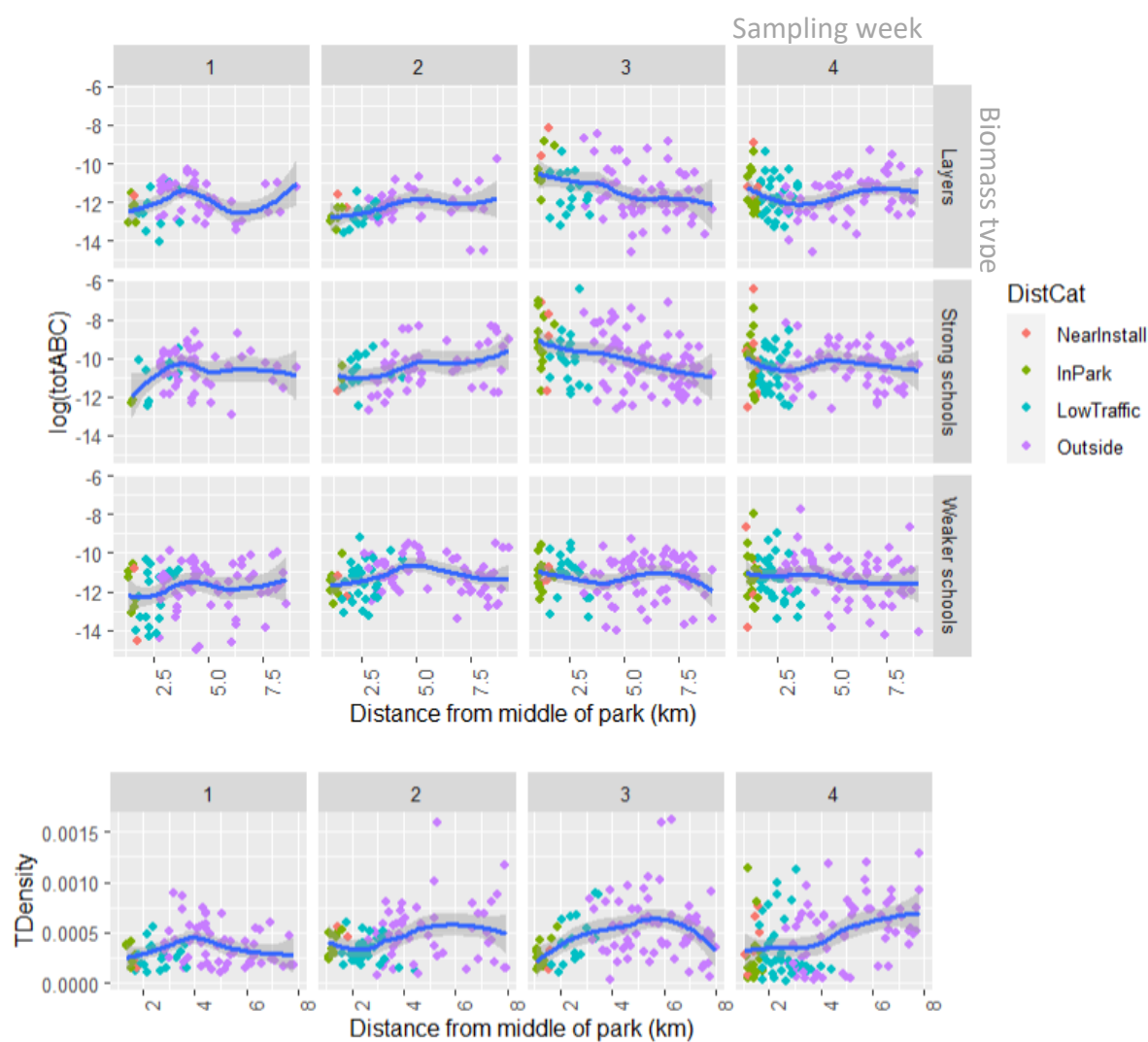


Figure 26 Weekly (1-4) temporal patterns in biomass or density index (y axis) by distance from the middle of the park (x axis) for zooplankton layers, strong and weaker fish schools (top three panel rows, in  $\log(\text{ABC})$ ) and for single fish targets (bottom panel row, in target density). The points are coloured by distance category (legend) and the loess smoothers (blue lines with grey shading for 95% CI) show the trend of the data.

When looking at distance categories, which are based on the minimum distance from any installation part (including anchoring chains), zooplankton in week 3 shows higher values within 100 m from the installations than elsewhere in the park area (Figure 27, top plot row).

This suggests the installations themselves may play a role in increasing zooplankton density, rather than the park as a complex. The density of single targets near the installations changed between weeks, but was always well within the range of the other categories, or lower (Figure 27, bottom plot row).

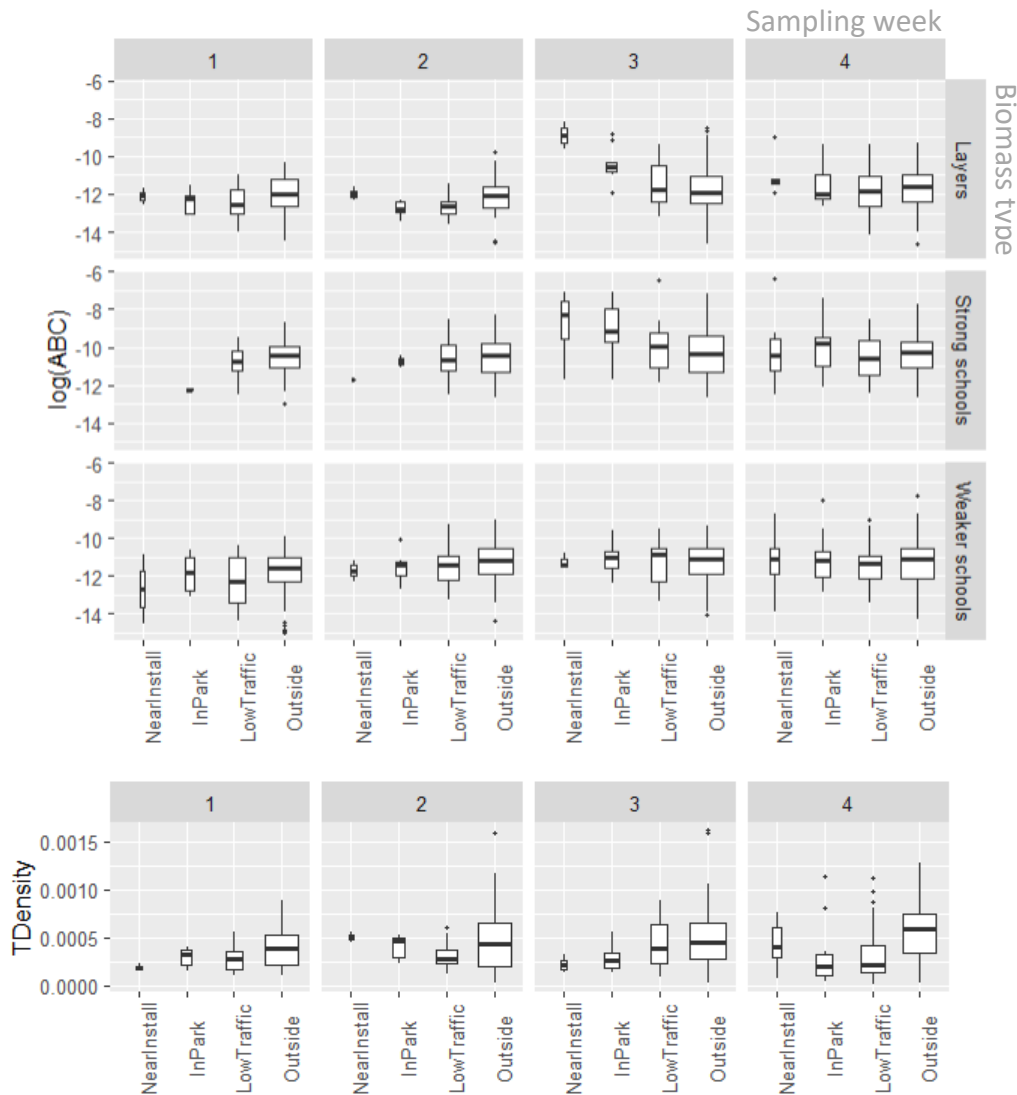


Figure 27 Weekly (1-4) temporal patterns in biomass or density index (y axis) by distance category (x axis) for zooplankton layers, strong and weaker fish schools (top three panel rows, in  $\log(ABC)$ ) and for single fish targets (bottom panel row, in target density). Distance categories are based on the minimum distance from any installation part.

The vertical distribution of layers and schools was on average deeper for the distance classes closer to the installations. When taking into account DVM, however, it was evident that this trend was mainly due to the higher incidence of transects close to the installations during daytime, when the biomasses are located towards the bottom. The biomass depth of the distance categories close to the park was always within the range of biomass depths of the Outside category (Appendix Figure 34).

## **Summary:**

A clear succession of primary and secondary producers was evident during the sampling month and was patchily distributed.

The biomass increase of schooling fish was synchronized with zooplankton peaks in time and space, suggesting a movement response to increased secondary production. The response was particularly evident for large zooplankton concentrations.

The installations likely have an effect on the size of the production of the lower levels of the ecosystem, with a consequent higher aggregation of fish. The park does not host a constant higher fish biomass.

Single targets, on the other hand, showed decreased densities closer to the park.

DVM patterns near the park are similar to the rest of the area.

### **3.4.4 Disturbance sources**

Assuming the infrastructure acts as a reef and sustains increased low trophic level production in its vicinity, we would expect a systematic decrease in fish abundance with distance from the infrastructure. However, reef-effect can also be caused by the need for protection (from predators or fisheries) and mediated by avoidance due to disturbance (such as noise due to marine traffic).

The results in this study show increased fish biomasses near the infrastructure during certain periods and as a consequence of the onset of primary production. However, the low traffic area never showed high fish biomasses at any time with respect to the Outside category, where both fishery and traffic are higher.

## 4 Conclusions

---

### 4.1 Is there a reef-effect at Hywind Scotland?

The temporal and spatial patterns highlighted in this work suggest that the installations likely have an effect on the low trophic levels (primary and secondary producers) in boosting production and consequently increasing standing stock, which in turn triggers fish aggregations. The results, on the other hand, do not support the theory of consistent increased fish biomasses in the vicinity of the park over time, but rather a stronger response to the natural occurrence of phytoplankton bloom and subsequent trophic cascade.

While a time lag between phytoplankton and zooplankton increase has been observed in this study, the high aggregation of fish was nearly simultaneous with the zooplankton increase, indicating that fish responded fast, likely by moving towards the areas of high zooplankton concentration for feeding. Aggregation for protection, due to lower disturbance or reduced fishing, would have led to relatively higher fish biomasses in the low-traffic area, which was not the case.

Fixed installations generate increased water mixing from the tidal currents passing by the vertical submerged part of the structures, causing downstream turbulence, and down- and up-welling (Cazenave et al 2016, Floeter et al 2017). We can assume that this is true also for floating turbines, given that a significant part of their body is submerged (~80 m for Hywind Scotland), often reaching beyond the pycnocline in stratified waters in summer (at about 20 m depth at Hywind Scotland) adding ‘anthropogenic’ vertical mixing on top of natural mixing (Dorell et al 2022). A likely increase in vertical water mixing, would weaken the stratification process, with a later onset and a shorter overall duration (Luneva 2019). The increased availability of nutrients to the surface coupled with potential periodic stratification and destratification events during the spring and summer season are likely to significantly increase, rather than limit, primary production, as modelled by Luneva (2019).

At the same time, the large number of filter feeders growing on fixed offshore installations have been shown to prey on phytoplankton with potentially negative effects on its concentration. It has, however, been hypothesized that, after filtration, nutrients bound in phytoplankton would be readily made available by pelagic remineralization of the detritus. By this mechanism, it is to be expected that filtration would sustain a longer bloom through faster nutrient recycling and support higher productivity in regions that receive nutrient-enriched and phytoplankton reduced water masses from offshore wind farm areas by currents (Slavik et al 2019). A parallel study at Hywind Scotland (Karlsson et al 2021) has demonstrated a high level of growth on the submerged parts of the turbine bodies and anchoring chains, as well as zonation and a succession process, with strong similarities to fixed turbines. We can therefore expect similar conditions with respect to nutrient levels at this floating park as in a complex of bottom fixed turbines.

This study was able to give insight on the relatively large-scale variability patterns of resources and did not investigate the potential fish aggregations at a spatial scale smaller than 100 m distance, for logistics reasons. Previous studies identified the highest aggregations of reef fish within 40 m from the installations (Vandendriessche et al. 2013). We can therefore not exclude from this study that an additional reef-effect on certain species exists at a very local scale ( $\ll$  100 m). Reef associated fishes, preying mostly on epibenthic hard substrate fauna, are not the same species detected in the dense schools in this study, which are most likely zooplankton-feeding pelagic fish. The latter are known to also aggregate under floating

devices not necessarily for feeding (Castro et al. 2002). In this particular case, we do not think that the floating turbines acted as aggregating devices (FAD) per se, but likely affected low trophic level pelagic production.

Due to the relatively low winds during the sampling season, the Sailbuoy's main course was largely influenced by the direction of the tidal current (Appendix Figure 36), potentially introducing a bias of oversampling the same water masses while sailing with the current. This bias would influence zooplankton abundances, drifting passively with the current, but likely not fish, which is able to actively swim to maintain position. The speed of the Sailbuoy, when sailing with the current, was on average 0.6 m/s (50% of data in 0.4 - 0.8 m/s range), while, when sailing against the current, it was on average 0.3 m/s (50% of data in 0.15 – 0.45 m/s range). In periods of low current (i.e. when the tide was turning) the speed of the Sailbuoy was still 0.5 m/s (50% of data in 0.3 - 0.6 m/s range), quite similar to the speed range with the current. This suggests that the wind propulsion had a large effect on the Sailbuoy speed, even though the current was determining the transect main directionality. Surface tidal currents in the area are relatively strong and are often higher than the Sailbuoy speed and occur mainly in the N/S direction (Figure 28). We can therefore assume that, even if the Sailbuoy was mainly sailing in the same direction as the currents, it was rarely drifting with the current at identical speed and was therefore not sampling the same water masses continuously.

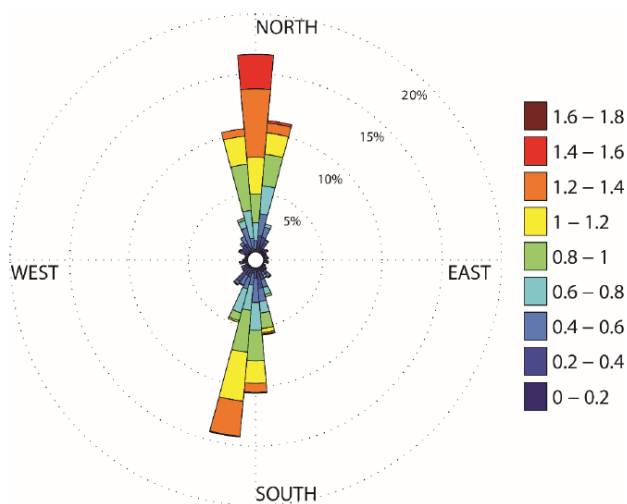


Figure 28 Current rose (colour scale: speed in m/s) at Hywind Scotland at 5 m depth, yearly average for 2019. Source European North West Shelf model provided by the UK- met-office.

Given that currents are mainly tidally driven in the area and reverse their direction approximately every 6h, we expected the effect of the park on the adjacent water masses likely to occur on the N/S axis and its range to be dependent on the current strength at any given period. We conclude that a current-dependent sampling design, as in this study, would increase the autocorrelation between successive samples on a N/S transect with respect to other directions and to times of lower current strength, but average values should not be affected. Moreover, the range of potential impact of the infrastructure, as for example the tail of high concentration of zooplankton south of the installations in Appendix Figure 35, should be considered as a maximum rather than an average, as it was sampled on a transect following a southward current.

One last caution should be taken in the interpretation of the results in this study with respect to the assessment of the effect of the wind park with respect to the generally highly productive deep waters of the Buchan Deep, where the park is located. As shown in this work as well (section 3.3.1), deep waters host generally higher biomasses with respect to neighbouring shallower areas. To ensure that the effect of the wind park on lower trophic level production is overall higher than the Buchan Deep area, and that these results are not just an isolated case during this particular year and period, repeated and longer studies should be performed, focusing particularly on the production season.

## 4.2 Suitability of the approach for offshore wind parks

The results from this study provided insight in a variety of temporal and spatial patterns of zooplankton and fish. The use of a glider technology allowed for:

- Long term sampling, allowing to harvest data for a relatively long period of time (ie. one month) and catch both repetitive (DVM) and non-repetitive patterns (bloom and successions) in a complex system
- Large range sampling, allowed for a wider range of environmental covariates, and longer gradients
- Autonomy, allowed for data sampling day and night (despite the biased spatial sampling outside the park at night for logistics reasons). DVM patterns are major sources of variation at mid latitudes.
- Fully unmanned remote operation, reducing risks on personnel

Despite the inability to perform a detailed fish species identification with the current data (an area which is currently under fast development), we were able to characterize different types of fish schools and distinguish between fish and zooplankton aggregations. Moreover, different schooling characteristics and depth distributions of fish corresponded to different movement patterns both vertically and horizontally with respect to the wind park. This providing further information on the potential species

The strongest temporal patterns were connected to daylight and related to the vertical migration of both fish and zooplankton. Vertical migrations encompassed the entire water column (down to 120m) for some group, but were close to inexistent for others. The choice of technology (transducer type and FM data collection) was successful in monitoring the entire water column, hence detect such patterns.

The effect of environmental variables (e.g. bottom depth) on the biomasses and densities was noticeable because of the wide area sampled. The original planned distance gradient was of up to 1 km distance from the infrastructures. However, due to logistical challenges on site, the Sailbuoy had to span a much wider area. This was beneficial to the campaign as it allowed us to pick up large spatial trends, that would have otherwise been undetected.

In this study, we chose to sample across distance gradients rather than choosing a control region to compare data to. This revealed to be a good strategy, in particularly in light of the high covariation between single fish density and bottom depth. Sampling across varied bottom depths allowed us to detect this covariation and select a set of appropriate control data points a-posteriori.

Simple sampling designs (e.g. effect vs. control) are undoubtedly very powerful when testing well defined hypotheses in controlled environments, such as laboratory experiments. In these settings, an effect vs. control design allows to detect the effect and its size, when everything else is kept constant. In field experiments however, controlling for all possible sources of

variation is nearly impossible. In the case of being able to measure all the relevant variables that may affect our results, we may still end up having covariation between relevant and irrelevant variables, hence not being able to disentangle the source of the effect. In ecosystem studies, such as the present one, we are moreover facing the situation of not knowing beforehand which environmental factor will be affecting the results. This makes the a priori choice of an appropriate control site a challenging task.

The combination of large spatial range and continuous long-term sampling allowed us to pick up the succession dynamics of phytoplankton bloom, followed by secondary production and by the likely aggregating response of large schools of fish to the patchy increased concentrations of zooplankton. The continuous sampling day and night gave insight in the different DVM patterns for different biological groups, something that would not have been possible with restricted sampling during the day.

For these reasons, we believe that sampling throughout a relatively large temporal and spatial range, as done in this case, was key in gathering valuable insight of complex patterns.

### **4.3 Suggestions for future investigations/applications**

The results in this study suggest a higher production of the lower trophic levels, in particular in the vicinity of the installations. This is explained by results from other studies on the role of biofouling in enhancing dissolved nutrients and in the changes in currents increasing mixing of the water column (Cazenave et al 2016, Floeter et al 2017).

These theoretical explanations could be tested by collecting data on oceanographic characteristics to inform hydrographic models on the current and turbulence regimes around the turbines. Glider and remote sensing technology exists to sample current data, microturbulence and dissolved nutrients.

The sampling approach in this study was able to detect large scale spatial patterns, but found higher biomasses in the data points collected within 100 m from the installations with respect to elsewhere in the park. This suggest that a very local effect of the installations can be expected. Moreover, different species than the highly aggregated pelagic schools detected in this study may be aggregating at even smaller spatial scales ( $\ll$  100 m, Vandendriessche et al. 2013) than the minimum for this study and may have remained undetected.

In order to obtain more precise estimates of the biomasses close to the infrastructure, further studies are suggested.

As partially shown in this study, but also outlined in the literature research, seasonality is likely affecting the extent of the effect of the installations on the environment. A similar approach in different seasons and multiple years would therefore be of interest to measure the inter-seasonal variability and understand the overall effect of the installations at sea, in particular with respect to the generally rich areas of the Buchan Deep. A longer sampling campaign from the start of the spring bloom to the end of summer would give deeper insight on possible multiple succession cycles through the season.

Small scale reef-effect on fish has been shown to be species-specific (Reubens et al. 2014). The current approach (i.e. lacking on site net/trawl sampling) was not able to provide clear information on different trends for different fish species and life stages. The technological developments around automatic species identification, from acoustic samples alone, is fast and promising. Following the improvement of detection algorithms, it may be possible in the near future to reanalyse the current dataset and provide more insight in species identification.

## 5 References

---

- Castro, J. J., Santiago, J. A., & Santana-Ortega, A. T. (2002). A general theory on fish aggregation to floating objects: an alternative to the meeting point hypothesis. *Reviews in fish biology and fisheries*, 11(3), 255-277.
- Cazenave P.W., Torres R., Allen J.I. (2016). Unstructured grid modelling of offshore wind farm impacts on seasonally stratified shelf seas, *Progress in Oceanography*, 145: 25-41, <https://doi.org/10.1016/j.pocean.2016.04.004>.
- Dorrell, R., Lloyd, C., Lincoln, B., Rippeth, T., Taylor, J., Caulfield, C. C., ... & Simpson, J. (2021). Anthropogenic Mixing of Seasonally Stratified Shelf Seas by Offshore Wind Farm Infrastructure. <https://doi.org/10.48550/arXiv:2112.12571>, preprint arXiv:2112.12571.
- Floeter J., van Beusekom J. E.E., Auch D., Callies U., Carpenter J., Dudeck T., Eberle S., Eckhardt A., Gloe D., Hänselmann K., Hufnagl M., Janßen S., Lenhart H., Möller K.O., North R.P., Pohlmann T., Riethmüller R., Schulz S., Spreizenbarth S., Temming A., Walter B., Zielinski O., Möllmann C. (2017). Pelagic effects of offshore wind farm foundations in the stratified North Sea, *Progress in Oceanography*, 156: 154-173, <https://doi.org/10.1016/j.pocean.2017.07.003>.
- Jakobsen H.H., Markager S. (2016) Carbon-to-chlorophyll ratio for phytoplankton in temperate coastal waters: Seasonal patterns and relationship to nutrients. *Limnology and Oceanography* 61(5): 1853-1868, <https://doi.org/10.1002/lno.10338>.
- Karlsson, R., Tivefålh, M., Duranović, I., Kjølhamar, A., and Murvoll, K. M. (2021) Artificial hard substrate colonisation in the offshore Hywind Scotland Pilot Park , *Wind Energ. Sci. Discuss.* [preprint], <https://doi.org/10.5194/wes-2021-123>, in review, 2021.
- Leonhard, S. B., Stenberg, C., Støttrup, J., Deurs, M. V., Christensen, A., & Pedersen, J. (2013). Fish benefits from offshore wind farm development. In *Danish offshore wind - key environmental issues – a follow-up* (pp. 31- 45). Danish Energy Agency.
- Lindeboom, H. J., Kouwenhoven, H. J., Bergman, M. J. N., Bouma, S., Brasseur, S., Daan, R., Fijn, R. C., De Haan, D., Dirksen, S., Van Hal, R., Hille Ris Lambers, R., Ter Hofstede, R., Krijgsveld, K. L., Leopold, M., & Scheidat, M. (2011) Short-term ecological effects of an offshore wind farm in the Dutch coastal zone; A compilation. *Environmental Research Letters*, 6(3).
- Luneva, M. V., Wakelin, S., Holt, J. T., Inall, M. E., Kozlov, I. E., Palmer, M. R., ... & Polton, J. A. (2019). Challenging vertical turbulence mixing schemes in a tidally energetic environment: 1. 3-D shelf-sea model assessment. *Journal of Geophysical Research: Oceans*, 124(8), 6360-6387.
- MacLennan, D. N., Fernandes, P. G., and Dalen, J. (2002) A consistent approach to definitions and symbols in fisheries acoustics. *ICES Journal of Marine Science*, 59: 365–369.
- Reubens, J.T., Degraer, S. & Vincx, M. (2014) The ecology of benthopelagic fishes at offshore wind farms: a synthesis of 4 years of research. *Hydrobiologia* 727: 121-136.
- Slavik, K., C. Lemmen, W. Zhang, O. Kerimoglu, K. Klingbeil, and K.W. Wirtz (2019). The large-scale impact of offshore wind farm structures on pelagic primary productivity in the southern North Sea. *Hydrobiologia* 845(1):35–53, <https://doi.org/10.1007/s10750-018-3653-5>.

- Soldal AV, Bronstad O, Humborstad O, Jørgensen T, Løkkeborg S, Svellingen I. 1998. Oil production structures in the North Sea as fish aggregating devices. Paper presented at: International Council for Exploration of the Sea. ICES CM 1998:U11.
- Vandendriessche, S., Reubens, J., Derweduwen, J., Degraer, S., & Vincx, M., Offshore wind farms as productive sites for fishes? In: Degraer, S., Brabant, R., & Rumes, B. (2013). Environmental Impacts of Offshore Wind Farms in the Belgian Part of the North Sea: Learning From the Past to Optimise Future Monitoring Programs. Royal Belgian Institute of Natural Sciences, Brussels, p 153-161.

## 6 Appendix

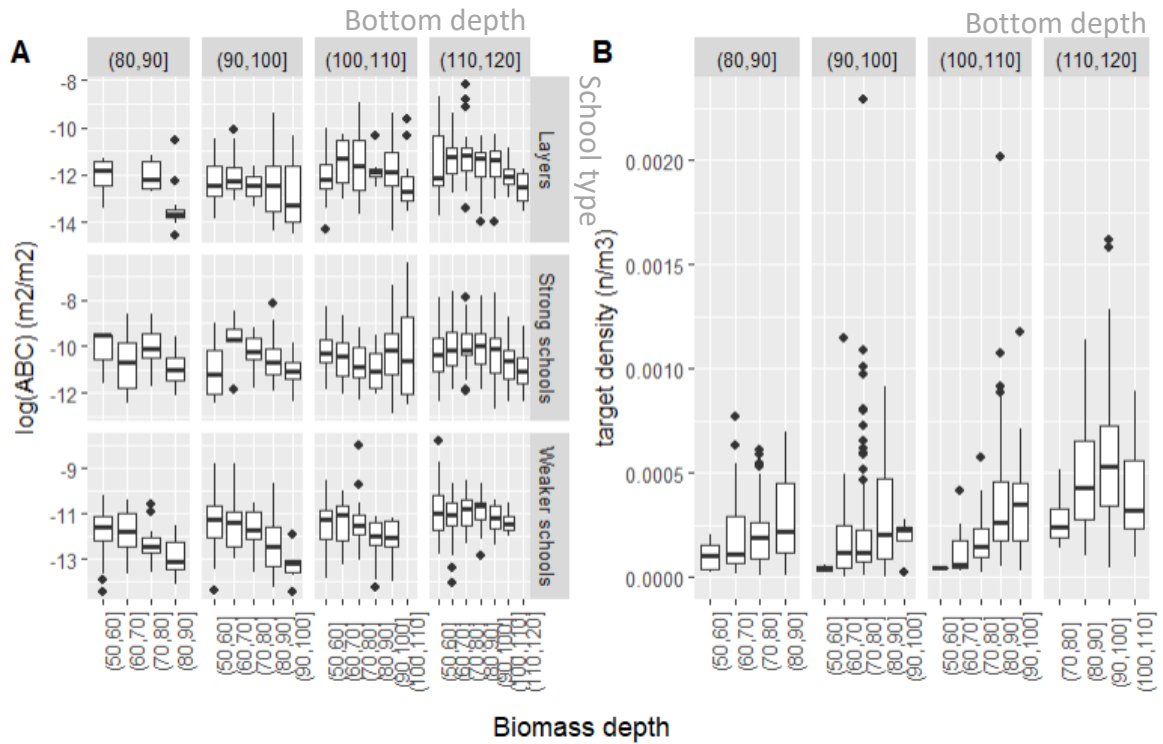


Figure 29 The patterns of different biomass of zooplankton layers and fish schools (A) and single fish targets density (B) with their depth in the water column (x axis) and the sample's bottom depth (panels). See 2.4.4 for specification on ABC and target density. All depths are shown in meters.

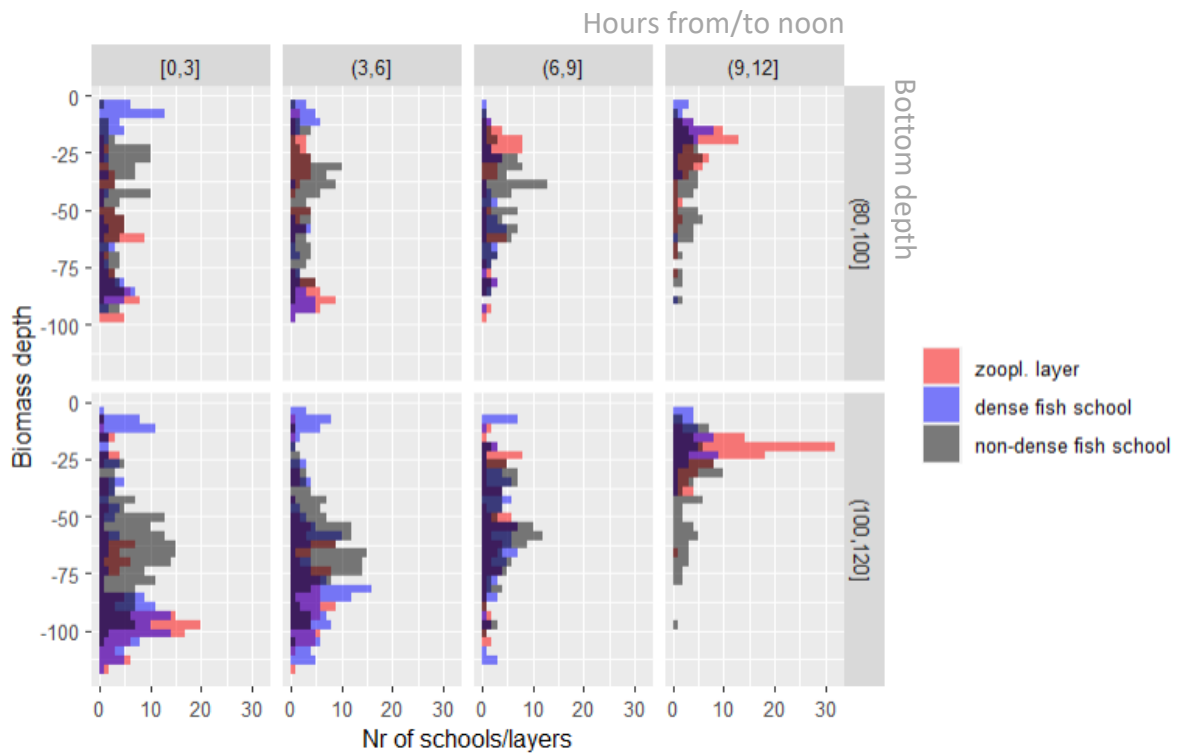


Figure 30 Frequency of occurrence (not total biomass) of different types of schools for two sets of samples with different bottom depth ranges (80-100m and 100-120m, plot rows) and for 4 times of the day (hours difference from/to noon 0-3h = from 9:00 – 12:00 & 12:00 - 15:00, 3-6h = 6:00 – 9:00 & 15:00 – 18:00, 6-9h = 3:00 – 6:00 & 18:00 – 21:00, 9-12h = 00:00 - 3:00 & 12:00 – 24:00). All depths are shown in meters.

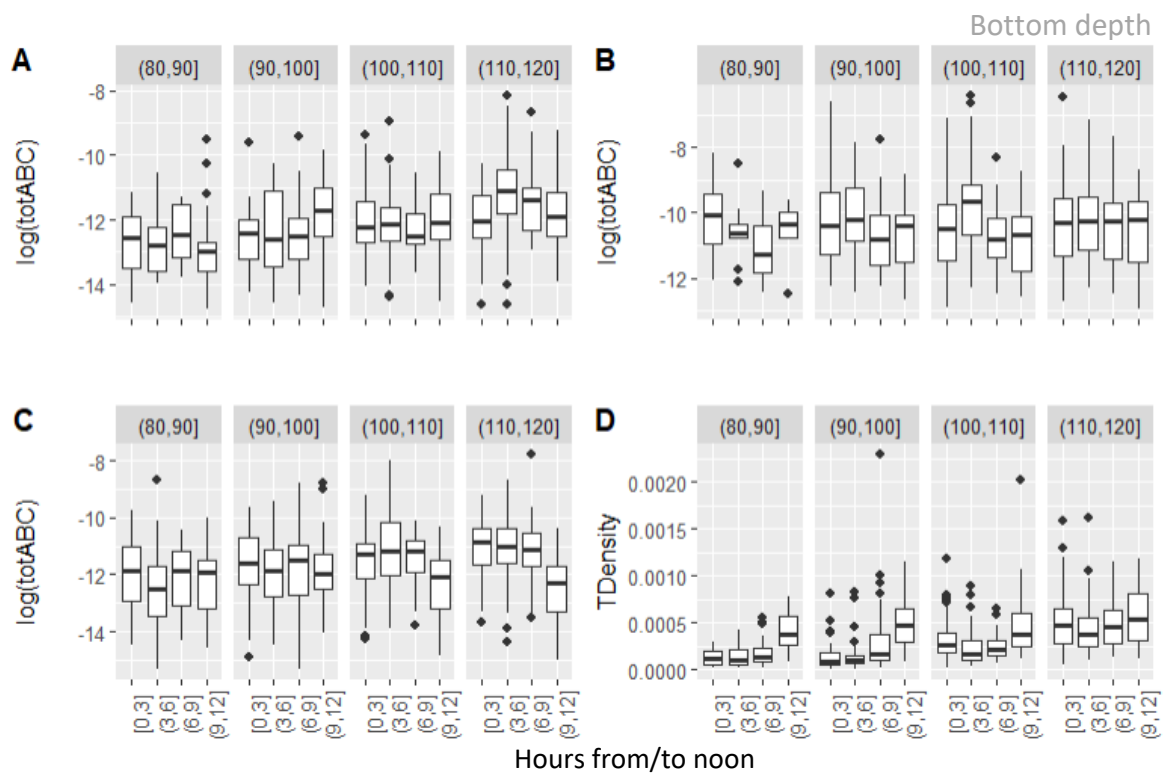


Figure 31 Biomass of zooplankton (A), non-dense fish schools (B), dense fish schools (C), and density of single fishes (targets, D) by time of the day (hours from/to noon, x axis), and by sample's bottom depth (panels). A, B and C show no consistent patterns with time of the day, within each depth category, while an increasing pattern is seen in D.

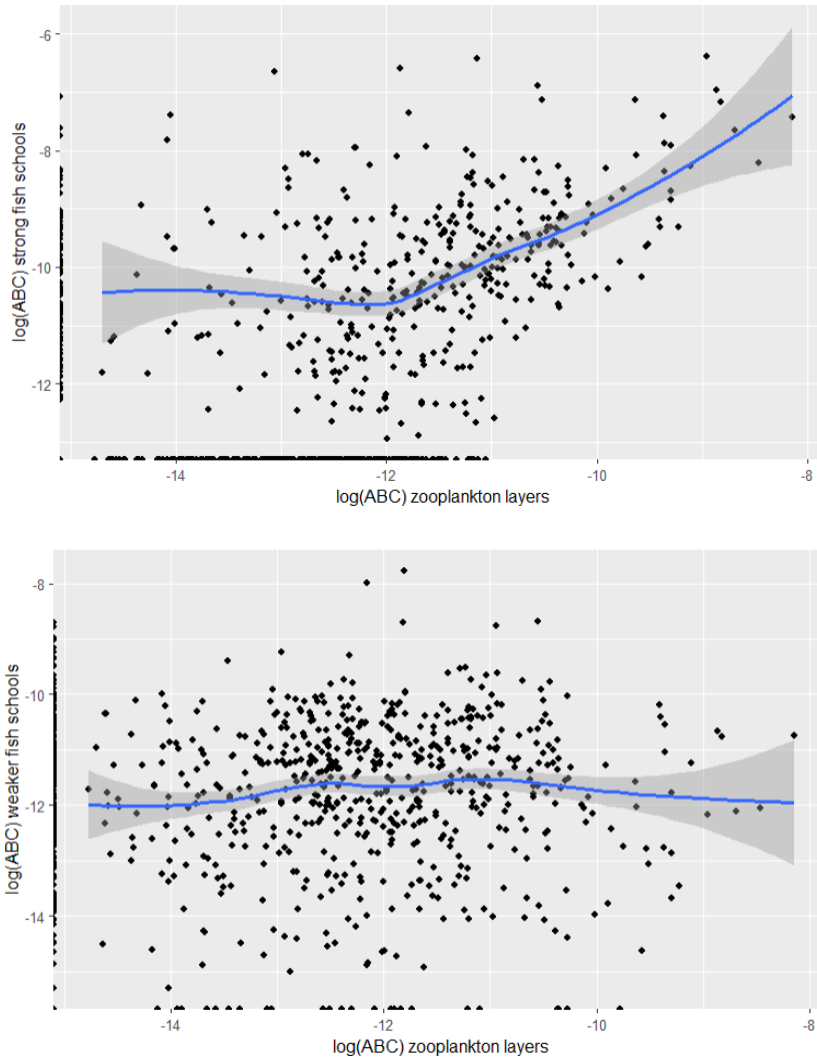


Figure 32 Relationship between the biomass indexes ( $\log(ABC)$ ) of zooplankton ( $x$  axis) and two types of fish schools (stronger signal, top panel, and weaker signal, bottom panel). Zooplankton and strong schools are positively related, in particular for higher aggregations of zooplankton ( $> -12 \log(ABC)$ ).

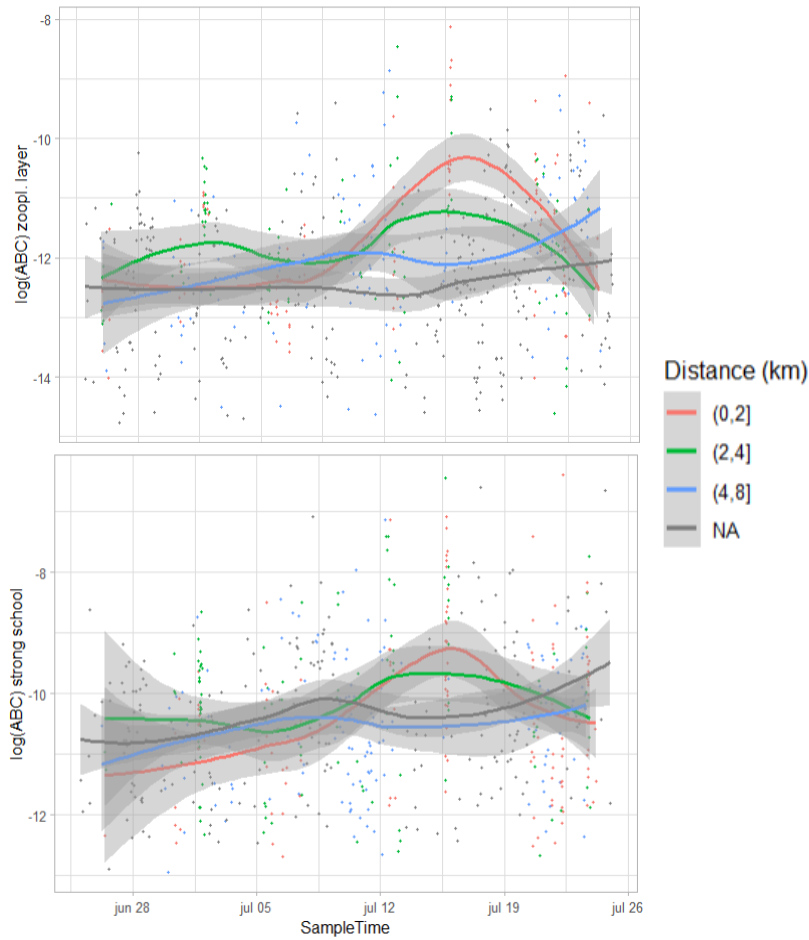


Figure 33 Trends in biomass ( $\log(ABC) \text{ m}^2/\text{m}^2$ ) of zooplankton (top panel) and strong schools of fish (bottom panel) at different distances from the park (loess smoothers). The smoothers show the data collected between 0-2, 2-4, 4-8 and beyond 8 km from the centre of the park (see colour legend). The peaks in each plots are higher for the data closer to the park (orange smoother).

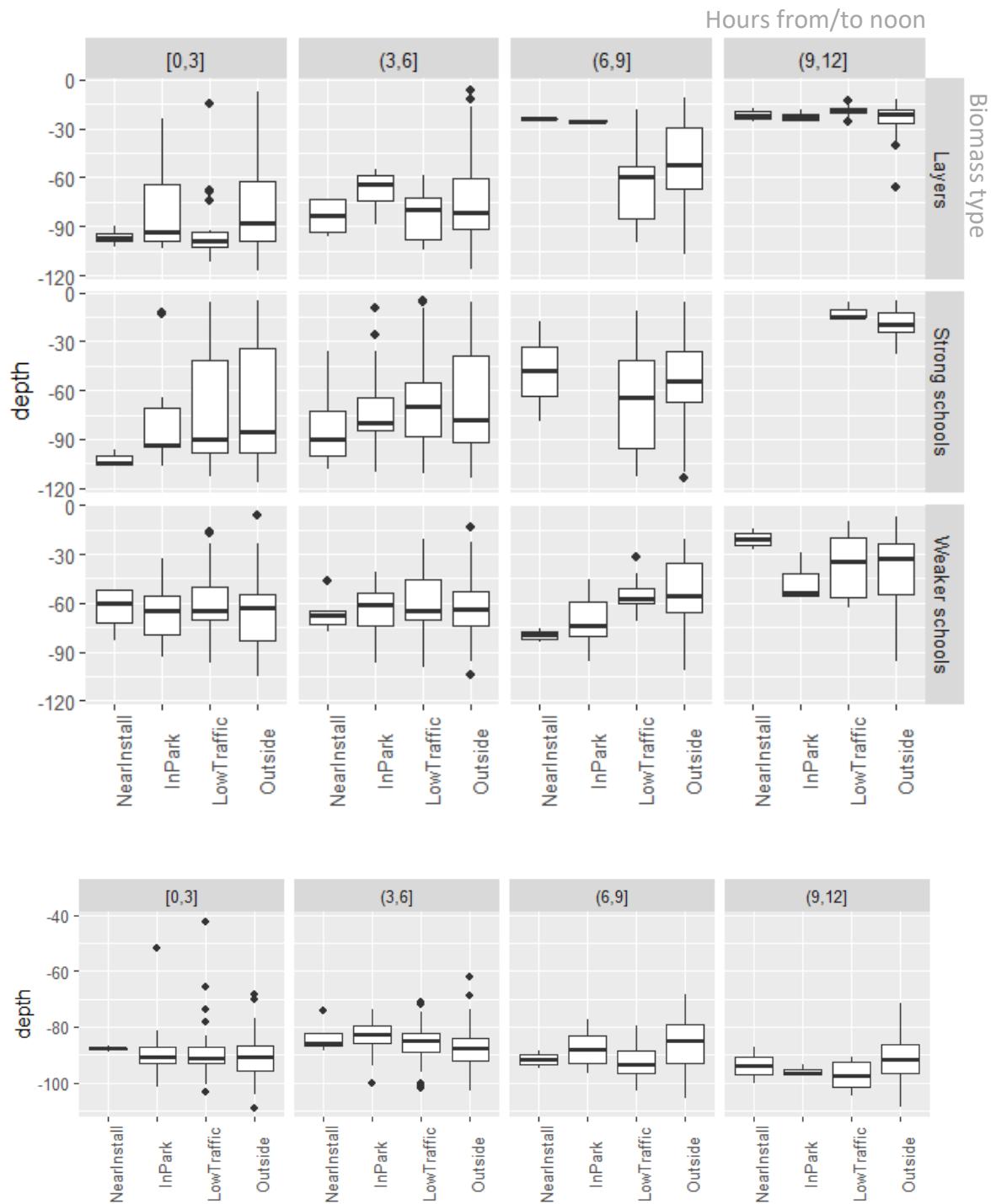
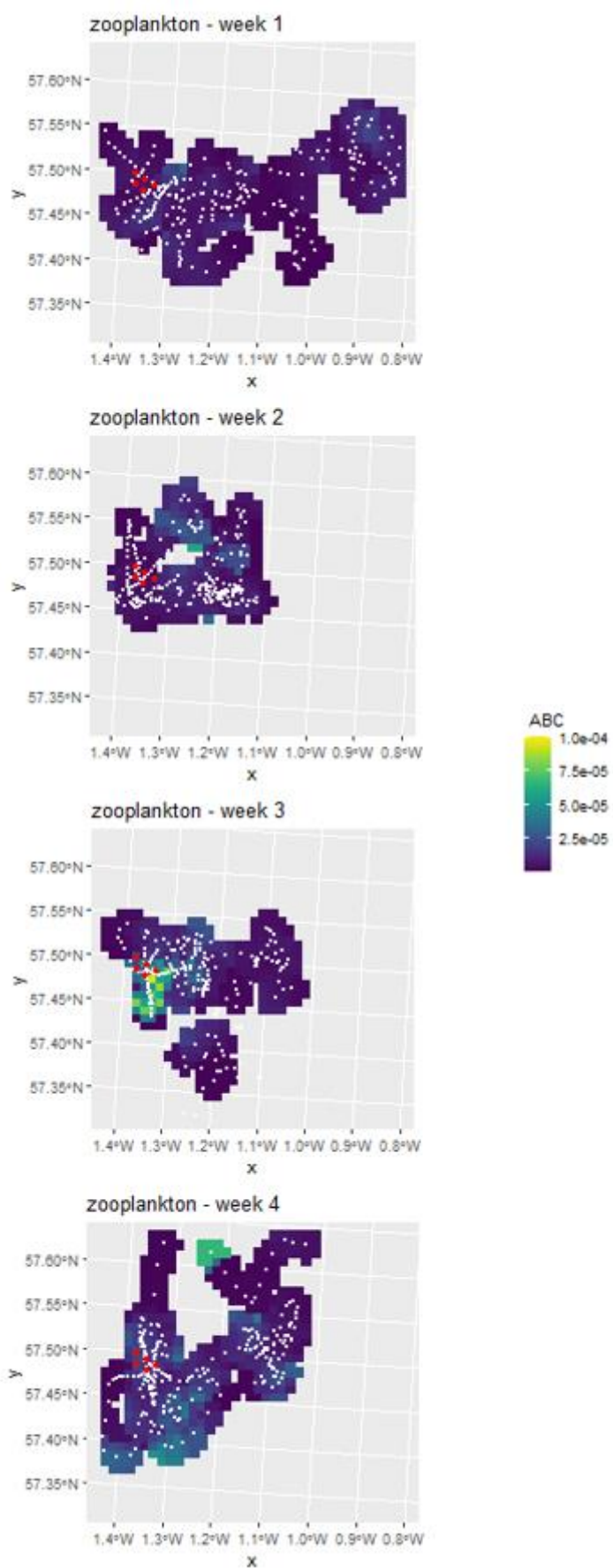


Figure 34 Biomass depth distribution by time of the day (panel columns, hours difference from/to noon 0-3h = from 9:00 – 12:00 & 12:00 - 15:00, 3-6h = 6:00 – 9:00 & 15:00 – 18:00, 6-9h = 3:00 – 6:00 & 18:00 – 21:00, 9-12h = 00:00 - 3:00 & 12:00 – 24:00) and distance categories (x axis). Panel rows show the different school types.



*Figure 35 Weekly spatial distribution of zooplankton in absolute values of ABC (colour scale) for week 1 and 3. The zooplankton distribution maps are spatially interpolated (by kriging, see 2.7 for details) and the location of the data samples (echograms) are shown as white dots. The five wind turbines are marked as red dots in all maps, together with the 100m depth contour lines (black) indicating the location of the Buchan Deep corridor (>100m).*

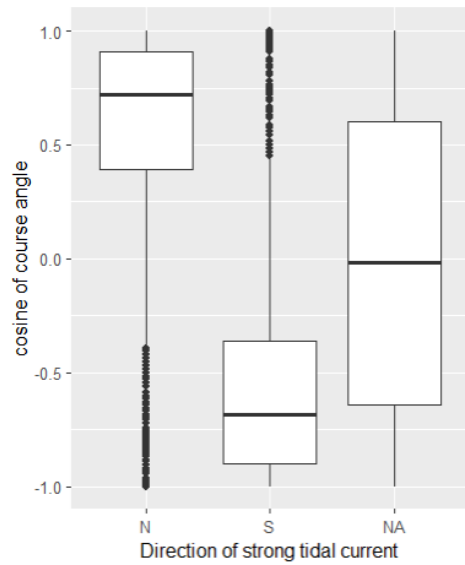


Figure 36 Direction of the Sailbuoy sampling track (y axis) in periods of strong northwards or southward tidal currents (N, S respectively, x axis) or lack of such (i.e. when the tide is turning, NA, x axis). The Sailbuoy direction is expressed in the cosine of its course angle to the north ( $N = \cos(0^\circ) = 1$ ,  $S = \cos(180^\circ) = -1$ ,  $E$  or  $W = \cos(\pm 90^\circ) = 0$ ).